Aqueous-Sulfate Stable Isotopes—A Study of Mining-Affected and Undisturbed Acidic Drainage

By D. Kirk Nordstrom, Winfield G. Wright, M. Alisa Mast, Dana J. Bove, and Robert O. Rye

Chapter E8 of
Integrated Investigations of Environmental Effects of Historical Mining in the Animas River Watershed, San Juan County, Colorado
Edited by Stanley E. Church, Paul von Guerard, and Susan E. Finger

Professional Paper 1651

U.S. Department of the Interior
U.S. Geological Survey

Contents

Figures

Tables

Chapter E8
Aqueous-Sulfate Stable Isotopes—A Study of Mining-Affected and Undisturbed Acidic Drainage

By D. Kirk Nordstrom, Winfield G. Wright, M. Alisa Mast, Dana J. Bove, and Robert O. Rye

Abstract

The combined results from major-ion chemistry and sulfur isotopes show three dominant processes affecting water quality: gypsum and anhydrite dissolution, pyrite oxidation, and calcite dissolution. This conclusion is based on more than one hundred samples including water, pyrite, gypsum, and anhydrite, collected in the Animas River watershed study area and analyzed for stable sulfur and oxygen isotopes ($\delta^{34}S$ in pyrite and $\delta^{34}S$ and $\delta^{18}O$ in aqueous sulfate and sulfate minerals).

Gypsum and anhydrite are shown to be dominantly hypogene (hydrothermal) in origin with heavy sulfur and oxygen isotopic compositions ($\delta^{34}S_{SO_4}$ =15 to 18 per mil and $\delta^{18}O_{SO_4}$ = –3 to 5 per mil). Pyrite is significantly lighter ($\delta^{34}S$= –7 to 2.5 per mil). Gypsum and anhydrite dissolution and pyrite oxidation are the dominant sources of dissolved sulfate in these waters. Distinct trends of mixing between water dominated by gypsum/anhydrite dissolution and water dominated by pyrite oxidation are inferred from the data.

A tendency for aqueous sulfate in water samples from unmined areas to have slightly higher $\delta^{18}O$ relative to aqueous sulfate in water from mined areas is also apparent in the data, although there is considerable dispersion in the values, with several overlapping data points. Part of this enrichment is caused by differences in isotopic composition originating from aqueous sulfate derived from different locations and alteration types. Another possible reason for this small enrichment in $\delta^{18}O$ in aqueous sulfate in pyrite oxidation-dominated waters might be the greater production of ferric iron in mined environments that leads to greater utilization of oxygen from the water molecule rather than molecular oxygen from air in the formation of aqueous sulfate. A distinct relationship between the $\delta^{18}O_{SO_4}$ values for pyrite oxidation-dominated waters and the $\delta^{18}O$ in water is not apparent, although the $\delta^{18}O_{SO_4}$ values are generally in a range that agrees with laboratory experiments. Evaporation, mixing of pyrite oxidation-dominated water with gypsum/anhydrite-dominated water, and dilution or mixing of water subsequent to pyrite oxidation are all important processes that can confound the interpretation of oxygen isotopic data from aqueous sulfate in mineralized and mined areas.

Introduction

The oxidation of pyrite is a complex hydrobiogeochemical process that adversely affects the water quality of receiving streams by producing acid waters with high metal concentrations. Sulfide ore extraction and processing, for gold, silver, copper, lead, and zinc production, enhances the rate of pyrite oxidation, increases the rate of acid production, and can cause severe environmental damage (Plumlee and Logsdon, 1999; Jambor and others, 2003). A considerable amount of research in the last decade has been applied to understanding, quantifying, and modeling the process of sulfide-mineral oxidation during weathering (Nordstrom, 2000; Nordstrom, 2004). The interpretation of stable isotope data of aqueous sulfate, SO_4^{2-}, derived from pyrite oxidation has been a challenging research topic and not well understood (van Stempvoort and Krouse, 1994; Taylor and Wheeler, 1994). Analyses of the stable isotope ratios of both sulfur and oxygen in sulfate have the potential to constrain the possible sources of sulfate and mechanisms of sulfide oxidation when stable sulfate isotopes are used in conjunction with the stable isotopes of water. For example, if pyrite is oxidized primarily by ferric iron, the oxygen in aqueous sulfate is derived from the water molecule as shown in equation 1:

$$FeS_2 + 14Fe^{3+} + 8H_2O \Rightarrow 15Fe^{2+} + 2SO_4^{2-} + 16H^+ \qquad (1)$$

Alternatively, if pyrite is oxidized by oxygen, only $^1/_8$ of the oxygen in aqueous sulfate is derived from the water molecule and the rest is derived from atmospheric oxygen as shown by equation 2:

$$FeS_2 + {}^7/_2O_2 + H_2O \Rightarrow Fe^{2+} + 2SO_4^{2-} + 2H^+ \qquad (2)$$

The large difference between $\delta^{18}O$ of air (+23.5°/$_{oo}$) and that of water (variable but generally –50 to +10 °/$_{oo}$ depending on distance from ocean, and on elevation, temperature, climate, latitude, and storm tracks) might provide a tool for distinguishing these two mechanisms. The very slow rate of oxygen isotopic exchange between sulfate and water (Lloyd, 1968) except at exceptionally low pH and (or) higher temperature (Hoering and Kennedy, 1957; Seal and others, 2000; Seal, 2003) would preserve the isotopic signature. The idea that oxygen isotopes could distinguish between microbial and inorganic oxidation was proposed by Taylor and others (1984a); this idea has encountered criticism (Toran and Harris, 1989), however, because the actual pathways of electron transfer are not well understood.

Equations 1 and 2 are also used to represent the indirect (equation 1) and direct (equation 2) mechanisms by which chemolithoautotrophic bacteria are thought to catalyze pyrite oxidation (Silverman, 1967; Sand and others, 2001). The indirect mechanism is one in which Fe^{3+} directly oxidizes pyrite and the role of the bacteria is to reoxidize the Fe^{2+} to Fe^{3+} in solution. In the direct mechanism, the bacteria adhere to the pyrite surface and directly oxidize the Fe^{2+} and the S^{-} in pyrite by some unknown enzymatic mechanism. Although the direct bacterial mechanism does not require that 87 percent of the oxygen in the sulfate ion must come from air oxygen (equation 2), this mechanism does allow it. In the bacterial mechanism, air oxygen could either be reduced to the oxygen in sulfate or to the oxygen in water. Part of the difficulty in identifying where the oxygen in sulfate originates is in knowing the mechanism by which bacteria utilize oxygen as the electron acceptor. The bacterial mechanism is important because, abiotically, the oxidation rate by Fe^{3+} is significantly faster than by O_2; without microbial catalysis it is difficult to see how molecular oxygen would contribute to the resultant sulfate ion. By contrast, stable isotopes of sulfur and oxygen have the potential to constrain sources. For example, many mineralized rocks also contain gypsum and anhydrite in addition to pyrite. The stable isotopes of sulfate might allow the discrimination between pyrite oxidation and gypsum/anhydrite dissolution as sources of the dissolved sulfate in ground water (for example, van Everdingen and Krouse, 1988; Nriagu and others, 1991). Stable isotope data on sulfate minerals whose parent aqueous sulfate formed from sulfide oxidation in natural, acidic weathering environments have been presented by Rye and others (1992) and Rye and Alpers (1997) in addition to the authors already mentioned.

Acknowledgments

Fieldwork and isotope determinations were made possible from the AML Initiative funding. The senior author is grateful to the National Research Program, WRD, for their support of this research. Thoughtful and thorough reviews by Robert R. Seal, II, Charles N. Alpers, and Craig Johnson are greatly appreciated and led to several improvements.

Purpose and Scope

This report presents and interprets sulfate stable isotope data for more than 100 water and mineral samples collected from the Animas River watershed study area in the San Juan Mountains near Silverton, Colo. The samples represent the consequences of weathering reactions in a variety of geologic and hydrologic conditions and cover a wide range of water composition (Mast and others, this volume, Chapter E7). The San Juan Mountains have undergone extensive hydrothermal alteration and mineralization (Bove and others, this volume, Chapter E3), allowing us the opportunity to collect samples from a variety of mineralized zones including both mined and unmined environments across a large area.

Study objectives were:

- To review the literature on pyrite oxidation and the use of sulfate stable isotopes for hypotheses and arguments from theory and experiments that would assist in the interpretation of field data
- To collect a large enough data set so that the factors controlling the isotopic signature of dissolved sulfate in these waters could be discerned, especially the origin of the sulfate oxygen
- To determine whether a different isotopic signature exists for acid drainage from mines than acid drainage from rocks undisturbed by mining
- To improve our understanding of pyrite oxidation through the application of isotopes.

Previous Studies

The complex pathways by which the sulfur in pyrite becomes sulfate in aqueous solution involve several intermediate steps that may be affected by temperature, pH, solution composition, and microbial metabolism and ecology (Lowson, 1982; Nordstrom and Southam, 1997; Nordstrom and Alpers, 1999; Nordstrom, 2000). The oxygen isotope composition of the sulfate is affected by the isotopic composition of the reacting substances (Krouse and others, 1991; van Stempvoort and Krouse, 1994). The sulfur moiety changes from an operationally defined oxidation state of 1– to 6+, or a transfer of seven electrons per sulfur atom. This electronic transfer cannot happen in a single step (Pearson, 1976) and, consequently, several intermediate sulfoxyanions are implicated during the oxidation (Nordstrom, 1982; Goldhaber, 1983; Moses and others, 1987). Several studies have brought insight to these pathways from chemical laboratory experiments, isotopic laboratory experiments, quantum-mechanical calculations, and field data. This section reviews these pathways and formulates hypotheses about the source of oxygen in the final sulfate ion that is needed for the interpretation of isotopic data of dissolved sulfate in samples from the Animas River watershed study area.

This review emphasizes recent investigations that reveal the nature of bonding of oxygen, whether from molecular oxygen or from water oxygen, to the sulfur in the pyrite surface and to reaction products such as thiosulfate and sulfite.

Inorganic Pyrite Oxidation

The initial attack on pyrite under oxic conditions and in the presence of water is a surface reaction that promotes a dissociative sorption of the water molecule at the pyrite surface, forming iron-oxygen bonds across the surface that are precursors to hydrous ferric oxide formation (Rosso and others, 1999). Iron oxyhydroxide surface formation clearly precedes sulfate formation (Nesbitt and Muir, 1994). The form of iron oxyhydroxide has been identified as goethite (at pH 9.2), and the coordination and bond distances have been measured at the pyrite surface after small amounts of reaction (England and others, 1999). Pseudomorphs of goethite after pyrite are well known and seem to have formed slowly at circumneutral to high pH. When surface coatings of hydrated ferric oxide are formed, ferrous iron in this oxide layer can more readily reduce molecular oxygen than the ferrous iron in pyrite can (Eggelston and others, 1996). Hence, experimental evidence indicates that molecular oxygen reacts initially with the iron and not with the sulfur in pyrite.

One of the consequences of iron-oxygen bond formation is to depopulate sulfur surface sites so that they become slightly more hydrophilic and more susceptible to the formation of sulfur-oxygen bonds (Rosso and others, 1999). The origin of the oxygen combining with the sulfur appears to be from water unless the primary hydration sphere of the oxidized iron transfers its oxygen to sulfur when Fe^{3+} oxidizes a reduced sulfur species (for example, Moses and Herman, 1991). The mechanism proposed by Moses and others (1987) involving the formation of a hydroxyl free radical from the hydration sphere of Fe(III) (the oxidant in experiments at low pH) has been experimentally verified by Bourda and others (2001, 2003) and further confirms that the oxygen that initially bonds to the iron and the sulfur is derived from the oxygen in water, not the molecular oxygen from air.

The oxidation of the sulfur, after the initial stage, is more complex because of the multiple sulfur species of intermediate oxidation state between 1– and 6+ that can form as proposed by Nordstrom (1982). Sato (1960) and Biegler and Swift (1979) used electrochemical measurements on pyrite in aqueous solution to show ferrous ions and the formation of either disulfide molecules or elemental sulfur. Bergholm (1955) was one of the first to carefully monitor pyrite oxidation in laboratory experiments and showed the formation of elemental sulfur and sulfate at temperature in excess of 50°C. One of the first studies to indicate thiosulfate formation on oxidizing pyrite is that of Steger and Desjardins (1978). Nesbitt and Muir (1994) monitored the initial reaction of pyrite with air and water vapor with X-ray photoelectron spectroscopy and found that the species disulfide, monosulfide, and polysulfide evolved through time (monosulfide decreasing, disulfide and polysulfide increasing) to eventually form sulfate and thiosulfate. Since then, Goldhaber (1983), Moses and others (1987), and Schippers and others (1996) have shown that thiosulfate, sulfite, and polythionates are all formed in different amounts depending on pH, oxidant, microbial ecology, and time.

Although the formation of intermediate sulfoxyanions has been measured during pyrite oxidation, the exact mechanism is still not entirely resolved. The consistent appearance of thiosulfate early in the reaction (those at low pH and without ferric ion as an oxidant) prompted Moses and others (1987) and Luther (1987, 1990) to postulate that a dioxygen molecule reacts directly with a disulfide molecule to form thiosulfate as the first dissolved sulfur oxidation product. At circumneutral pH, it was postulated that the dioxygen molecule reacted with reduced iron and then the oxidized iron provided an electron sink for electrons to leave reduced sulfur. At low pH, ferric ion can oxidize pyrite under anoxic conditions (Garrels and Thompson, 1960) so that all of the oxygen in sulfate must come from the water molecule.

An important question is whether air oxygen or water oxygen is used during the oxidation of sulfoxyanion intermediates to sulfate. Thiosulfate oxidizes to tetrathionate in the presence of pyrite (Xu and Schoonen, 1995) or Fe^{3+} (Williamson and Rimstidt, 1993), and tetrathionate tends to decompose through a series of reactions that include the production of trithionate, pentathionate, trisulfane monosulfonic acid or disulfane monosulfonic acid, and sulfite before ending with sulfate (Schippers and others, 1996; Druschel, Hamers, and Banfield, 2003; Druschel, Hamers, and others, 2003). Apparently, the only stages of the reaction that might require molecular oxygen are in the decomposition of tetrathionate to sulfate and in the oxidation of sulfite to sulfate. Druschel, Hamers, and Banfield (2003) suggested that the overall oxidation of tetrathionate in the presence of oxygen and ferric ion can be represented by:

$$S_4O_6^{2-} + 3Fe^{3+} + {}^{11}/_{4}O_2 + {}^{9}/_{2}H_2O \Rightarrow 3Fe^{2+} + 4SO_4^{2-} + 9H^+ \quad (3)$$

If it is assumed that all of the oxygen in tetrathionate is derived from the water molecule, then reaction 3 would dictate that about 34 percent of the oxygen in sulfate could be from molecular oxygen. This amount of molecular oxygen is in the range that Gould and others (1989) found in their isotopically controlled sulfide mineral oxidation experiments. Tetrathionate oxidizes through microbial mechanisms that generally do not require molecular oxygen, and the breakdown of polythionates by known enzymes is possible (de Jong and others, 1997; Friederich, 1998) in *Acidithiobacillus ferrooxidans* and *Acidithiobacillus thiooxidans* (formerly *Thiobacillus ferrooxidans* and *Thiobacillus thiooxidans*, Kelly and Wood, 2000). The most recent review summarizing information on the enzymatic oxidation of elemental sulfur to sulfate can be found in Kelly (1999). Polythionates are more stable than sulfite (Druschel,

Hamers, and Banfield, 2003; Roy and Trudinger, 1970). Sulfite is another decomposition product of both thiosulfate and polythionates and the immediate precursor to sulfate. The enzymatic decomposition of tetrathionate produces thiosulfate and elemental sulfur (de Jong and others, 1997), both of which will further oxidize to sulfate. As mentioned previously, Schippers and others (1996, 1999) have outlined complex microbial pathways for the oxidation of tetrathionate, polythionates, polysulfane monosulfonic acids, and thiosulfate to sulfate. Recent work by Druschel, Hamers, and others (2003) has shown that the formation of hydroxyl radicals, known to occur on the pyrite surface in the presence of water, can oxidize polythionates much faster than molecular oxygen or Fe(III). They concluded that reaction with hydroxyl radicals is the only inorganic pathway for polythionates to oxidize to sulfate. The reaction appears to involve a trisulfane monosulfonic acid intermediate that can then further decompose in the presence of molecular oxygen to produce sulfur monoxides and sulfite and finally sulfate. These reactions would only allow molecular oxygen to be accommodated in the final sulfate by oxidation of sulfite to sulfate.

Sulfite oxidizes rapidly to sulfate in the presence of oxygen (Ermakov and others, 1997), but it oxidizes more rapidly by 2- or 3-fold in the presence of ferric ion (Brandt and van Eldik, 1998; Millero, 2001). Oxidation by ferric ion would not require any molecular oxygen, although studies by Holt and others (1981, 1983) indicate stoichiometric contributions of molecular oxygen during sulfite oxidation without iron. The amount of molecular oxygen may well be a function of pH, wherein more molecular oxygen appears in the sulfate at higher pH because of the insolubility of ferric iron (Seal, 2003). Furthermore, the oxygens in sulfite are known to exchange quickly with water oxygen (Hall and Alexander, 1940; Betts and Voss, 1970) so that sulfite might only contain water oxygen regardless of its previous history. Hence, if the last stage of sulfur oxidation always involves the oxidation of sulfite to sulfate, then the primary pathway for molecular oxygen to enter the sulfate ion is during this reaction. The amount that enters will depend on pH, Fe(III) concentrations, oxygen concentrations, and possibly temperature.

Processes Contributing to Sulfate Stable Isotope Compositions in Mineralized Areas

Hydrothermal sulfide and sulfate minerals in mineral deposits generally have sulfur isotopic compositions that vary in the range of –10 to +25 per mil (Clark and Fritz, 1997; Faure, 1986; Krouse and Mayer, 2000; Seal and others, 2000) with sulfide minerals commonly in the range of –10 to +10 per mil and sulfate minerals having values significantly higher. Little fractionation of sulfur appears to take place during weathering to produce aqueous sulfate. Field (1966) hypothesized that the $\delta^{34}S$ of sulfides would change little on oxidation to sulfate and reported data that suggested fractionation effects of –2 to +3 per mil. This conclusion has been supported by studies of supergene alunite (Rye and others, 1992) and jarosite (Rye and Alpers, 1997) from numerous ore deposits. Toran and Harris (1989) summarized most of the extant literature and confirmed, from both lab studies and field studies, that not more that a few per mil fractionation takes place during oxidation of S_2^{2-} in pyrite to S^{6+} in dissolved sulfate.

The stable isotopes of sulfate should be a useful constraint for interpreting the operative processes of pyrite oxidation, especially at mining sites, if different source minerals had different sulfur isotope compositions and if the reaction pathways of molecular versus water oxygen are reflected in the oxygen isotopes of sulfate. Two complications make these interpretations challenging, however. First, there can be four general sources of sulfate in addition to pyrite oxidation: sulfate mineral dissolution, atmospheric sulfate, residual sulfate after partial reduction, and recycled sulfate (re-oxidized after reduction). Hypogene sulfate minerals are commonly associated with many sulfide deposits and need to be considered in any isotope study (Toran, 1987). Sulfate mineral dissolution, especially from gypsum and anhydrite, will be shown to be a major process in the Animas River watershed. In our study area, atmospheric sulfate in precipitation is very low in concentration relative to that found in most acid water and can be considered negligible. Cycling of sulfur through redox reactions is critical for some coal mine drainage situations and cannot be discounted in our study, but it seems unlikely to be a major process affecting sulfate stable isotopes in mountainous metal-sulfide deposits of the western United States. Water samples were collected in areas of high elevation and steep topography, and drainages did not infiltrate large wetlands. Small, localized wetlands were encountered in a few places and were not likely to have had significant effects on the sulfate stable isotopes. Second, an exchange of ^{18}O–^{16}O between aqueous sulfate and water can occur where special hydrologic conditions permit long residence times in low-pH environments (Chiba and Sakai, 1985; Alpers and others, 1992; Seal and others, 2000; Seal, 2003). But the samples in this study are unlikely to have sufficiently low pH and sufficiently long residence time to permit isotope exchange. Evidence of long-term ponding is not evident in the water stable isotope data.

Generalized Isotope Mass Balances on Sulfate

Several possible mechanisms exist by which both atmospheric oxygen and water oxygen can be incorporated into the final sulfate from pyrite oxidation. Assuming the stoichiometry of reactions 1 and 2, and assuming contributions from the dissolution of sulfate minerals, the contributions of each type of oxygen will follow the isotope mass balance equation:

$$\delta^{18}O_{SO_4} = Y\{X(\delta^{18}O_w + \varepsilon_w) + (1-X)[0.875(\delta^{18}O_a + \varepsilon_a) + 0.125(\delta^{18}O_w + \varepsilon_w)]\} + (1-Y)\,\Sigma_m\, x_m(\delta^{18}O_m) \qquad (4)$$

where X=the fraction of sulfate oxygen from the water (w) molecule by reaction 1 with the remainder (1–X) coming from air (a) oxygen from reaction 2, and with ε_w and ε_a the fractionation factors for water and air, respectively (van Everdingen and Krouse, 1985; van Everdingen and others, 1985; van Everdingen and Krouse, 1988; Toran and Harris, 1989; Clark and Fritz, 1997) and Y=the fraction of pyrite-derived sulfate with the remainder (1–Y) coming from the sum of the fractions (x) of dissolved sulfate minerals (m) and their isotopic compositions. As long as no oxygen isotopic exchange takes place between dissolved sulfate (from minerals) and the water molecule, there will be no fractionation factor. The complicating factors are

1. the mechanism by which microbes affect the transfer of oxygen
2. the mechanism by which unstable or metastable intermediate sulfoxyanion formation affects the isotopic composition
3. the variability in $\delta^{18}O_{H_2O}$ from climatic conditions, and
4. the extent to which $\delta^{18}O_{H_2O}$ actually represents the composition of the water that reacted with the pyrite at the site of oxidation (that is, complications from evaporation and from mixing of waters of different $\delta^{18}O_{H_2O}$ after oxidation occurred).

Equation 3 is linear and can be rearranged and simplified to give an empirical function of $\delta^{18}O_{H_2O}$:

$$\delta^{18}O_{SO_4} = m(\delta^{18}O_{H_2O}) + b \quad (5)$$

where the contributions from soluble sulfate minerals can be neglected, the atmospheric oxygen contribution is considered constant or can be determined by difference after the water-oxygen dependence has been ascertained, b is an empirical intercept, and where the fraction of water oxygens, m=0.875X+0.125. Hence, a plot of $\delta^{18}O_{SO_4}$ against $\delta^{18}O_{H_2O}$ could be solved for the proportion of reaction 1 versus reaction 2. Alternatively, if the fractionation factors are known, a diagram can be constructed with lines for varying proportions of these reactions and field data can be plotted on them. Both approaches have been utilized in previous studies (for example, van Everdingen and others, 1985; van Everdingen and Krouse, 1988).

Biotic and Abiotic Oxygen Isotope Studies on Sulfate Formation from Reduced Sulfur Oxidation

Several different lab experiments using O_2 or H_2O of known isotopic composition help to constrain the reaction mechanisms of sulfate formation. Lloyd (1967) found that sulfate formed from the bacterial oxidation of hydrogen sulfide incorporated 64–76 percent of its oxygen from water and the remainder from atmospheric oxygen. No significant fractionation was observed when water oxygen was incorporated, but a fractionation of –8.7 per mil was observed for atmospheric oxygen.

A strong dependency of sulfate $\delta^{18}O$ on the $\delta^{18}O$ of the water molecule was found in several experiments involving sulfur or sulfide mineral oxidation. Mizutani and Rafter (1969) oxidized elemental sulfur in two waters of different oxygen isotope composition using wet silty soil as a bacterial source. The results showed no fractionation, that is, $\delta^{18}O_{SO_4}$ had the same value as $\delta^{18}O_{H_2O}$.

Microbial oxidation of reduced sulfur compounds has been investigated for many decades, and yet the biochemical processes by which sulfur-oxidizing autotrophic bacteria gain energy are not clearly elucidated. Depending on what the processes are, atmospheric oxygen may or may not be incorporated into the final sulfate ion. Microbial sulfur-oxidizing activity is caused by one or more enzymes, generally called sulfur (or sulfide) oxidases. An oxidase is any enzyme that catalyzes an oxidation reaction. If an enzyme catalyzes the incorporation of O_2 into organic compounds (which then may contribute the oxygen to the formation of sulfate), then it is known as an oxygenase. Much of the research on the biochemistry of sulfur- and sulfide-oxidizing microbes has been directed toward characterization of these enzymes and whether they behave as oxygenases (Kelly, 1982, 1999). The general picture of oxidation of sulfide and sulfur by acidithiobacilli (Madigan and others, 2000) is that the reduced sulfur combines with a sulfhydryl group of the cell, such as glutathione, which is then oxidized to sulfite (with or without molecular oxygen) by a sulfide oxidase. The sulfite can further oxidize to sulfate by a sulfite oxidase. Electrons are captured from the electron donor, such as pyrite or sulfur, and then transferred through an electron transport system (ETS) to the terminal electron acceptor, such as oxygen. The ETS is located in the membrane and includes a sequence of cytochrome enzymes which have been identified and studied in several thiobacilli. Adenosine triphosphate (ATP), the primary energy carrier in living organisms, is synthesized from adenosine diphosphate by the ETS. If the dominant sulfide-mineral-oxidizing bacteria operate with an ETS, then one would expect $\delta^{18}O_{SO_4}$ to be unaffected by $\delta^{18}O_2$ of air. With oxygenase, no metabolic energy is gained but $\delta^{18}O_{SO_4}$ is affected by isotopic composition of atmospheric oxygen.

Suzuki (1965) investigated the oxidation of sulfur by *Acidithiobacillus thiooxidans* and found that the resulting sulfate incorporated no ^{18}O from the air. A small amount of atmospheric oxygen was found when he used cell-free enzyme extracts, leading him to tentatively identify the sulfur-oxidizing enzyme as an oxygenase. Numerous enzymatic studies, reviewed most recently by Kelly (1999), have attempted to better characterize sulfur oxidation pathways among the thiobacilli. Oxygenases have been clearly demonstrated to be active in Archaea such as *Acidianus brierleyi*, a hypothermophile and acidophile. An important point was made that, although thiobacilli have in common the oxidation of reduced

sulfur to sulfate, different species appear to have different pathways. Kelly's review did not settle the relative importance of oxygenase and the ETS, but it did give lines of evidence indicating alternative explanations. He also pointed out that the use of oxygenase during sulfur moiety oxidation would reduce the possible sources of metabolic energy gain but it would increase the apparent efficiency of the energy by 2- to 3-fold. A revealing statement from Kelly (1999) provides a method for resolving the dilemma: "As yet, no attempt appears to have been made to determine the contribution in vivo of a sulfur oxygenase by providing bacteria with ^{18}O-labeled oxygen or water to determine the relative contributions of each to the oxygen recovered in the sulfate produced by oxidation of sulfur (and thiosulfate). It is possible that exchange reactions might obscure the involvement of any direct oxygenation." For the case of sulfide mineral oxidation, such studies have been reported but only rarely with the inclusion of controlled microbial catalysis.

Schwarcz and Cortecci (1974) found no correlation between the $\delta^{18}O$ of the dissolved sulfate and that of spring and stream waters of northern Italy and concluded that evaporite mineral sources, pyrite oxidation occurring at different temperatures and pH values, and isotopic fractionation of the molecular oxygen were all confounding factors that could cause the $\delta^{18}O_{SO_4}$ to vary independently of $\delta^{18}O_{H_2O}$. They did, however, show that pyrite oxidation in water of varying $\delta^{18}O$ caused a correlated increase of 0.6 per mil in the $\delta^{18}O_{SO_4}$ for every per mil increase in $\delta^{18}O_{H_2O}$. This study was one of the first to demonstrate that at least half of the oxygen in the sulfate was derived from the water molecule. Bailey and Peters (1976) conducted pyrite oxidation experiments with ^{18}O-labeled water at temperatures of 85°–110°C and found that 73–100 percent of the sulfate oxygen came from water oxygen. Taylor and others (1984a) found evidence for increases in $\delta^{18}O_{SO_4}$ with increasing in $\delta^{18}O_{H_2O}$ in acid mine waters from the western United States, but possible contributions from other sulfate mineral sources were not considered. Between 23 and 100 percent of the sulfate oxygen apparently originated from water oxygen in the experiments of Taylor and others (1984b) depending on the conditions of the experiments (anaerobic versus aerobic, sterile versus inoculated with *Acidithiobacillus ferrooxidans*). Van Everdingen and others (1985) estimated that 37–74 percent of the sulfate oxygen from various field locations was derived from water. Van Everdingen and Krouse (1988) also found 29–100 percent of the sulfate oxygen derived from water oxygen in lab experiments and 35–90 percent in field studies. They showed a plot of $\delta^{34}S_{SO_4}$ versus $\delta^{18}O_{SO_4}$ that suggested a mixing line involving dissolution of anhydrite, and when combined with the known occurrence of anhydrite at their field site (Pine Point, Northwest Territories), the isotopic data strongly implicate anhydrite as contributing to the more positive $\delta^{18}O_{SO_4}$ values. Cunningham and others (2005) showed similar mixing of aqueous sulfate derived from oxidation of pyrite and the dissolution of gypsum and alunite.

Gould and others (1989) demonstrated the consistent incorporation of water oxygen for a series of six experiments with four sulfide minerals (pyrite, chalcopyrite, sphalerite, and pentlandite) in nine different initial compositions of $\delta^{18}O_{H_2O}$, pH=2.5, and with *A. ferrooxidans.* The percent water oxygen was 23–80 overall but averaged 66–71 percent for the pyrite runs. They noted that an increase occurred in the proportion of incorporated water oxygen with time, and that the molecular oxygen was likely incorporated into a sulfoxyanion intermediate during the reaction. Further work by the same group (Krouse and others, 1991) demonstrated clearly that O_2 is incorporated into SO_4^{2-} during sulfide mineral oxidation. They only looked at the oxidation of pentlandite $(Fe,Ni)_9S_8$, a monosulfide; these results, thus, may not be comparable to pyrite oxidation because it is recognized that monosulfides oxidize differently in acid solutions than disulfides do. Monosulfides readily form H_2S, so that the oxidation process is similar to the oxidation of H_2S. Oxidation of H_2S under aerobic conditions proceeds by reacting with molecular oxygen (Zhang and Millero, 1994). Furthermore, as pointed out by Krouse and others (1991), even though molecular oxygen is needed to oxidize sulfite (an intermediate during the oxidation of any reduced inorganic sulfur compound), there is rapid ^{18}O–^{16}O exchange between H_2O and SO_3^{2-} (Betts and Voss, 1970; Eigen and others, 1961; Lloyd, 1967). The factors that control the isotopic exchange rate between these species are not well known, but Holt and others (1981) found that atmospheric oxygen contributed typically 25 percent or one of the four oxygen atoms in the sulfate molecule. Rapid isotopic exchange with water accounts for the remainder. These results could explain the fairly consistent trend of about 25–40 percent molecular oxygen occurring in sulfate from sulfide oxidation studies (Taylor and Wheeler, 1994; van Stempvoort and Krouse, 1994; Krouse and Mayer, 2000).

Reedy and others (1991) determined the proportion of actual isotopomers ($S^{16}O_n{}^{18}O_{4-n}$) produced during pyrite oxidation at pH 1 and 70°C and at pH 7 and 20°C by using vibrational spectroscopy and pure $^{18}O_2$ and pure $H_2{}^{16}O$ (and the reverse, pure $^{16}O_2$ and pure $H_2{}^{18}O$) for initial reactant compositions. Runs with and without Fe^{3+} were completed. They found that the water oxygen dominated the composition of the sulfate but that some atmospheric oxygen was present; that is, when they used pure $H_2{}^{16}O$, the sulfate was dominated by $S^{16}O_4$ but some $S^{16}O_3{}^{18}O$ was found. They also pointed to the oxidation of sulfite by O_2 and rapid exchange of sulfite oxygen with water oxygen. Consistent with other studies, they also found that the longer the experiments were run, the more water oxygen was found in the sulfate. Reaction kinetics clearly play an important role in the isotopic composition of oxygen in sulfate derived from pyrite oxidation.

The implication from these studies is that sulfite or polythionates are potentially the dominant, oxygen-isotope-controlling intermediates in the overall oxidation reaction. In a review of atmospheric studies of oxygen isotope behavior

during the air oxidation of SO_2 by Cunningham and others (1984), the isotopic composition of aerosol sulfate formed from the oxidation of SO_2 is composed of one air oxygen and three water oxygens. The lab and field results of atmospheric sulfate formation demonstrate clearly that it makes no difference what the oxygen isotope composition of the SO_2 is, the composition of the oxidation product, SO_4^{2-}, is composed of one air oxygen and three water oxygens (Holt and others, 1981). This conclusion favors the reactions,

$$SO_{2(g)} + ½O_{2(g)} = SO_{3(g)} \quad (6)$$

and

$$SO_{3(g)} + H_2O_{(l)} = H_2SO_{4(aq)} \quad (7)$$

that results in the isotopic relation

$$\delta^{18}O_{SO_4} = 0.75(\delta^{18}O_{H_2O}) + k \quad (8)$$

where k is a semi-empirical constant that can be derived from equation 4 if all the factors are known. If the sulfite ion (hydrolyzed SO_2) is a necessary intermediate to SO_4^{2-} formation during pyrite oxidation, and one oxygen in sulfite is always derived from molecular oxygen, then a constant 75 percent ratio of water oxygen might be expected. Note that in the sulfide mineral oxidation experiments of Gould and others (1989), the SO_4^{2-} approached 75 percent water oxygen at the longest times for four of the six runs. Although many of the experimental studies give results in this range, they do not consistently occur in this range. In the oxidation of pyrite, however, $SO_{2(g)}$ is not the main product formed, only aqueous sulfite ion in the presence of water, so the question is: by what pathway is sulfite formed? During H_2S oxidation by oxygen, an SO_2 radical is formed which then hydrolyzes and oxidizes, forming thiosulfate, sulfite, and ultimately sulfate (Zhang and Millero, 1994). If thiosulfate forms directly from the attack of molecular oxygen on the disulfide in pyrite, then there should be two oxygen atoms derived from atmospheric oxygen. The second alternative is, if rapid exchange of water oxygen with the sulfite ion occurs, then there should be only one atmospheric oxygen atom. The third alternative is, if ferric ion dominates the oxidation of sulfite, that there should be no atmospheric oxygen atoms. These limits might provide the actual controls on the sulfate-oxygen isotopic composition. That is, the range of water oxygen in sulfate oxygen would be 50–100 percent. This range is observed for experimental studies and for many field studies.

Sulfite ion oxidizes to sulfate rapidly in the presence of oxygen:

$$SO_{3(aq)}^{2-} + ½O_{2(g)} = SO_{4(aq)}^{2-} \quad (9)$$

Studies by Schippers and others (1996), Schippers and others (1999), Sand and others (2001), Druschel, Hamers, and Banfield (2003), and Druschel, Hamers, and others (2003) have shown that multiple complex pathways are likely involved with the intermediate stages of oxidation of the sulfur moiety from pyrite to sulfate. These pathways include formation of thiosulfate, polythionates, elemental sulfur, disulfane-monosulfonic acid, trisulfane-monosulfonic acid, and sulfite. These intermediate sulfoxyanions are likely to exchange their oxygen rapidly with water oxygen, but polysulfane-monosulfonic acids, like sulfite, might incorporate atmospheric oxygen during oxidation to sulfate. This possibility could also lead to larger $\delta^{18}O_{SO_4}$ values.

A brief recapitulation is needed. Whereas lab studies indicate some consistency in the relationship between $\delta^{18}O_{SO_4}$ and $\delta^{18}O_{H_2O}$, applying this information to field studies may be hindered by three important aspects. First, as pointed out by several researchers (Schwarcz and Cortecci, 1974; van Everdingen and others, 1985; Krouse and Mayer, 2000), dissolution of sulfate minerals, especially gypsum and anhydrite, must be quantitatively determined if they are part of the sulfate pool. Second, the H_2O in which the sulfate is dissolved may not have been the ambient H_2O at the time of pyrite oxidation. Evaporation and mixing with different waters can change $\delta^{18}O_{H_2O}$ without affecting $\delta^{18}O_{SO_4}$. Third, oxygen isotope exchange can occur between SO_4^{2-} and water in low-pH waters at elevated temperatures (Chiba and Sakai, 1985). Without a detailed analysis of the hydrology and mineralogy of every site, the interpretation of the isotopic data may not be well enough constrained. The additional possibility of cyclic reduction and re-oxidation in areas of bogs, wetlands, soils, or collapsed anoxic mines might also confuse the interpretation.

Field Area—Bedrock Mineralization and Alteration

The Animas River watershed study area is underlain primarily by intermediate volcanic rocks of Tertiary age that are hydrothermally altered and mineralized to varying degrees (Bove and others, this volume). A regional propylitic alteration affects nearly all rocks in the study area (Burbank and Luedke, 1969; Bove and others, this volume). The propylitic rocks are characterized by varying amounts of chlorite, epidote, calcite, and illite, in the presence of fresh to weakly altered primary feldspar crystals. Sparse, very fine grained pyrite also is common in the alteration assemblage. These weakly altered rocks were subjected to several generations and types of more intense alteration and mineralization. Studies by Bove and others (this volume) have delineated five different areas of the watershed that represent these different styles and ages of mineralization and alteration. Sampling locations and ranges of $\delta^{34}S$ for the dissolved sulfate are shown relative to these areas in figure 1. Some of these locations fall outside the five area boundaries and are generally associated with characteristics of both the Eureka Graben and South Silverton mineralized areas. A few others have similarities to Red Mountain but also

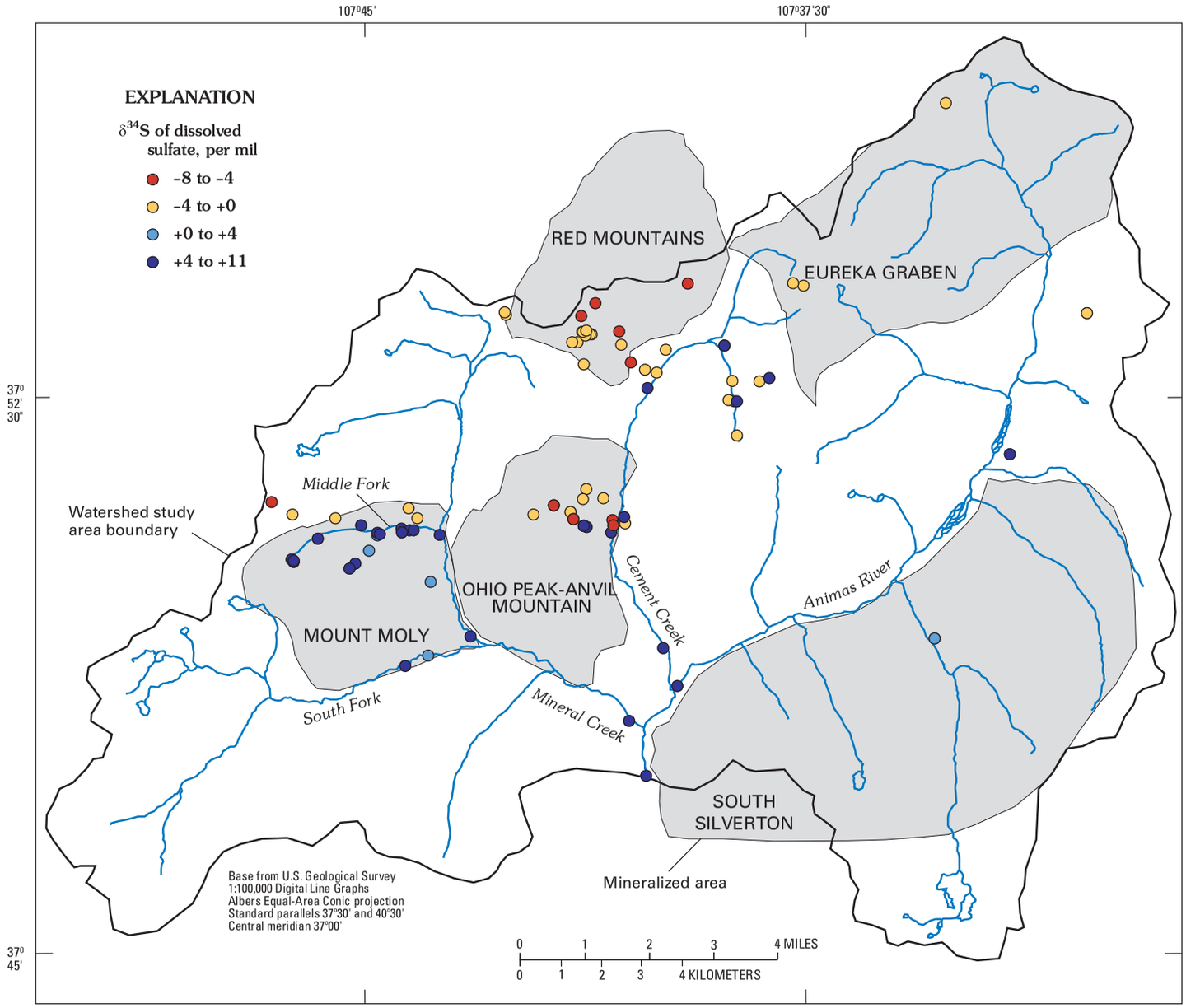

Figure 1. Animas River watershed study area, showing sampling site locations and distribution of $\delta^{34}S$ values of dissolved sulfate in surface water. Extent of five outlined mineralized areas defined by Bove and others (this volume, Chapter E3). Note that "Mount Moly" was used by Bove and others to name a mineralized area but is not a formal geographic name.

contain other overlapping mineralization. The five mineralized areas, which include Mount Moly[1], Red Mountains, Ohio Peak–Anvil Mountain, Eureka Graben, and South Silverton, are discussed briefly in the following section. For a more detailed discussion of these mineralized areas, the reader is referred to Bove and others (this volume). Aqueous sulfate in different types of altered areas shows different ranges and average isotopic compositions in figure 1. The sulfur-bearing mineralogy of these mineralized and altered areas varies, as does the local hydrology, and together these aspects undoubtedly affect the fine-scale isotopic composition of aqueous sulfate in a given drainage.

Hydrothermal alteration in the Mount Moly area was associated with quartz-monzonite intrusive activity that produced subeconomic copper-molybdenum porphyry mineralization (Bove and others, this volume). In the center of this area is a zone of quartz-sericite-pyrite (QSP) altered rock that grades outward into weak sericite-pyrite and propylitic zones. Rocks in the QSP zone are composed of coarse-grained sericite, secondary quartz, and fine-grained pyrite (2–5 volume percent). Drill core data indicate that gypsum is present in thin veins and fractures below the oxidized surface of the QSP zone. Mineralization in the Mount Moly area produced quartz-molybdenite stockwork veins, which are present in the QSP zone, and pyrite-quartz veins, which are present on the margins of the hydrothermal system. Barite is found as vein fillings, and coarse-grained gypsum also is found in the pyrite-quartz veins.

Intrusion of high-level dacite porphyry in the Red Mountains and Ohio Peak–Anvil Mountain areas resulted in extensive zones of acid-sulfate alteration (Burbank and Luedke, 1969; Bove and others, this volume). The acid-sulfate assemblage is composed of quartz, alunite, pyrophyllite, dickite, and as much as 30 volume percent pyrite. Broad expanses of QSP-altered rocks also are present between the acid-sulfate centers. Abundant veins and veinlets of anhydrite are present at depth within the QSP and potassic assemblages but are absent within the acid-sulfate zones. In the Red Mountains area, mineral deposits consist of silver-copper-lead-arsenic ores hosted within breccia pipes and brecciated fault zones (Burbank and Luedke, 1969; Bove and others, this volume). By contrast, the Ohio Peak–Anvil Mountain system is largely devoid of significant mineral deposits.

The Eureka Graben and South Silverton areas are characterized by 18–10 Ma vein mineralization that appears to be spatially and perhaps genetically related to intrusions of high-silica alkali rhyolite (Bove and others, this volume). Veins are mostly a polymetallic variety (silver, lead, zinc, copper, ±gold) and formed as fracture or fissure-fillings in the propylitic country rock. Many of these veins in the Eureka graben area are especially rich in manganese silicate gangue minerals. Vein and fracture-filling anhydrite and gypsum are also associated with the manganese-rich ores. Selenite (large clear blades of gypsum) after anhydrite is common in fractures throughout the watershed. Zones of hydrothermally altered rock related to these veins consist of narrow envelopes that are superimposed over regionally propylitic-altered rock. In some areas with high vein concentrations, the associated alteration zones can be locally pervasive.

This brief geologic overview provides a context for two important aspects of interpreting the stable sulfate isotope data: the mineralogy or source material and the spatial distribution of that source material. Sulfides, especially pyrite, are prominent throughout the Animas River watershed study area, and gypsum and anhydrite are also prominent in many places. Both of these sources contribute to the dissolved sulfate concentration of the surface and ground water. The remainder of this report focuses on the collection, measurement, and interpretation of the sulfate stable isotope data in the study area.

Methods

Water-Quality Sampling Methods

Water-quality samples for dissolved constituent and stable isotope analyses were collected at more than 80 stream, spring, and inactive mine sites in the study area during low-flow conditions from 1994 to 1999. Most samples were collected in the Middle Fork Mineral Creek subbasin of the Mineral Creek basin, and the Prospect Gulch, Ohio Gulch, South Fork Cement Creek, and Topeka Gulch subbasins of the Cement Creek basin (table 1; fig. 1). Field measurements, including stream discharge, specific conductance, pH, and water temperature, were made at sampling sites using methods described by Wilde and Radtke (1998). Field meters were calibrated in the morning on the day of the sample collection. The pH meter was calibrated with pH 2 and pH 4 buffers or pH 4 and pH 7 buffers to bracket the range of pH values measured in the field. The specific-conductance (SC) meter was calibrated with two standards that bracketed the range of values expected at the sampling sites. Instantaneous discharge was measured using a current meter according to methods described by Rantz and others (1982). Samples for dissolved constituents were field filtered into 250 mL polyethylene bottles using disposable 0.45 µm cartridge filters. Sample aliquots for calcium and total-iron analyses were preserved with 1 mL of concentrated nitric acid, and aliquots for ferrous iron analyses were preserved with 1 mL of 6M HCl. Unpreserved filtered aliquots were collected for sulfate determination. Unfiltered samples for stable isotopes of water were collected in 60 mL glass bottles with polyseal caps. Samples for sulfur and oxygen isotopes of sulfate were filtered into 1 L polyethylene bottles and preserved with 1 mL of 6M HCl.

[1]Mount Moly is the informal name for the peak referred to in this volume as peak 3,792 m. Its use in this report is confined to repetition of the name given by Bove and others (this volume, Chapter E3) to the altered and mineralized area around that peak and does not indicate a formal geographic name for peak 3,792 m.

Table 1. Chemical and isotopic data for non-mining affected and mining-affected samples collected in the Animas River watershed study area.

[Cat, category 1, no evidence of mining activity at site; 2, a site that appears to be unaffected, but is not unequivocal; 3, a site that is not directly impacted, but where upgradient mining activity likely affected the water quality; 4, direct discharge from mining activity at site. Calcium, sulfate, ferrous and ferric iron concentrations given in milligrams per liter, mg/L; --, no data; Q, discharge in cubic ft per second, cfs; Field Spec. Cond., specific conductance measured in the field, expressed in microsiemens per centimeter, µS/cm]

Site Number	Description	Date	Sample type	Cat	Q cfs	Field Spec. Cond. µS/cm	Field pH	Water temp. °C
CC1	Upper spring, Cement Creek	4/25/97	Spring	1	0.22	1,266	3.06	21.4
CC126	Spring in Topeka Gulch	9/2/94	Spring	1	0.030	835	3.77	7.4
CC127	Tributary of Topeka Gulch	9/2/94	Stream	1	0.040	642	3.56	12.4
CC128	Spring in Topeka Gulch	9/3/94	Spring	1	0.010	975	2.90	6.7
CC129	Topeka Gulch upstream from unnamed mine	9/3/94	Stream	1	0.15	558	3.27	9.0
CC130	Ferricrete spring in Topeka Gulch	9/4/94	Spring	1	0.001	437	4.32	7.5
CC131	Tributary of Topeka Gulch	9/4/94	Stream	1	0.002	575	3.49	17.6
CC132	Topeka Gulch upstream from MS73	9/9/94	Stream	1	0.030	500	3.45	10.3
CC32	South Fork Cement Creek downstream from Velocity Lake	10/17/96	Stream	1	0.43	150	7.10	3.0
CC36	Spring downstream from Red Mountain # 3 in Prospect Gulch	9/8/97	Spring	1	0.005	654	3.25	1.1
CC44	Spring in Prospect Gulch	9/9/97	Spring	1	0.020	685	6.40	1.6
CC45	Spring in Prospect Gulch	9/9/97	Spring	1	0.012	78	3.80	7.8
CC50	Spring in Ross Basin	9/5/97	Spring	1	0.001	87	6.92	2.2
CC51	Spring in Ross Basin	9/5/97	Spring	1	0.010	287	6.96	1.2
CC52	Spring in South Fork Cement Creek	10/18/96	Spring	1	0.031	520	3.95	1.8
CC53	Spring near Corkscrew Pass	9/7/97	Spring	1	0.010	76	3.92	11.2
CC70	Stream in Prospect Gulch	9/10/97	Stream	1	0.055	158	6.83	10.0
CC86	Upper Georgia Gulch	9/25/97	Stream	1	0.282	316	6.54	9.2
MC38	Spring southwest of Ohio Peak	8/9/99	Stream	1	--	1,340	2.58	--
MC61	Moss Bog spring near peak 3,792 m	8/26/97	Spring	1	--	304	4.20	12.3
MC62	Iron Bog spring near peak 3,792 m	8/26/97	Spring	1	--	659	3.45	8.5
MC69	Upper Red tributary	9/19/95	Stream	1	1.1	298	4.92	6.7
MC71	Spring in Red tributary	9/19/95	Spring	1	0.001	1,480	3.06	6.3
MC72	Small stream in Red tributary	9/19/95	Stream	1	0.17	881	3.12	13.4
MC74	Red tributary at mouth	9/20/95	Stream	1	1.6	1,087	3.39	3.8
MC76	Crystal Lake outflow	9/18/95	Stream	1	0.50	60	4.47	9.9
MC77	Spring near Ophir Pass	9/18/95	Spring	1	0.020	156	5.32	1.8
MC81	Moraine spring in Paradise basin	10/11/95	Spring	1	0.34	451	6.84	1.8
MC82	Spring in upper Paradise basin	10/11/95	Spring	1	0.070	1,845	5.72	5.5
MC83	Sulfide spring in Paradise basin	10/11/95	Spring	1	0.050	1,630	5.43	6.6
UA40	Spring near Houghton Mountain	9/4/98	Spring	1	0.019	609	3.95	0.6
UA40	Spring near Houghton Mountain	9/4/98	Spring	1	0.019	609	3.95	0.6
CC29	Red spring, lower Prospect Gulch	2/12/97	Spring	2	0.28	707	3.01	3.8
CC34	Spring above Big Colorado mine	10/18/96	Spring	2	0.46	295	3.75	4.1
CC57	Stream in Prospect Gulch	9/9/97	Stream	2	0.008	608	2.98	8.6
CC71	Stream in Prospect Gulch	9/26/97	Stream	2	0.18	365	6.90	4.8
MC30	Battleship Slide spring near peak 3,792 m	8/28/97	Spring	2	0.001	576	3.02	15.8
MC85	Spring in Middle Fork Mineral Creek	9/19/95	Spring	2	0.020	182	6.83	8.7
MC86	Spring in Middle Fork Mineral Creek	9/14/95	Spring	2	0.020	106	6.56	4.3
CC40	Spring in Middle Fork Cement Creek	10/1/97	Spring	3	0.045	195	3.77	3.8
CC69	Stream in Prospect Gulch	9/10/97	Stream	3	0.020	428	3.50	8.0
A68	Animas River at Silverton	2/25/97	Stream	4	18	360	6.90	0.1
A68	Animas River at Silverton	2/25/97	Stream	4	18	360	6.90	0.1
A72	Animas River downstream from Silverton	2/26/97	Stream	4	65	642	4.90	0.7
A72	Animas River downstream from Silverton	2/26/97	Stream	4	65	642	4.90	0.7
C48	Cement Creek at Silverton	9/29/94	Stream	4	17	1,040	3.94	9.6
CC100	Seep below Yukon tunnel dump	5/15/97	Spring	4	--	5,480	2.57	10.4
CC133	Topeka Gulch downstream from MS73	9/9/94	Stream	4	0.17	1,530	7.22	7.6

Table 1. Chemical and isotopic data for non-mining affected and mining-affected samples collected in the Animas River watershed study area.—Continued

$d^{18}O_{H_2O}$	dD_{H_2O}	$d^{18}O_{SO_4}$	$d^{34}S_{SO_4}$	Calcium mg/L	Sulfate mg/L	Molar Ca/SO_4 ratio	Ferrous iron mg/L	Total iron mg/L	Percent charge balance
–16.1	–117	0.90	6.80	160	634	0.61	--	38.5	–15.3
–16.3	–117	–4.40	–3.20	75	480	0.37	38.6	45.0	–10.0
–15.7	–114	–4.70	–1.50	56	370	0.36	25.5	31.0	–11.7
–16.2	–118	–6.20	–3.80	48	400	0.29	0.80	13.0	–9.3
–15.4	–111	–5.90	–5.10	31	190	0.39	2.9	13.0	6.5
–16.5	–121	–3.90	–6.60	69	290	0.57	20.0	20.0	0.4
–15.6	–116	–3.70	–6.70	55	230	0.57	0.10	0.67	–2.7
–15.0	–110	–6.80	–4.80	38	190	0.48	1.5	3.6	–0.8
--	--	–3.10	–1.50	22	33	1.64	0.006	<0.03	27.0
--	--	–5.60	–4.10	35	238	0.35	0.87	5.2	4.7
–15.8	–112	–7.80	–1.90	111	320	0.83	0.012	0.048	–24.6
–16.4	–121	–6.40	–4.90	6	32	0.47	0.49	0.69	9.6
--	--	--	0.00	13	28	1.10	--	<0.030	–8.2
--	--	--	–0.40	42	113	0.89	--	<0.030	–3.9
--	--	–2.30	–0.20	88	175	1.20	0.043	0.073	46.0
--	--	--	–4.60	1	25	0.14	--	<0.030	–43.3
–14.9	–107	–5.40	–0.60	23	72	0.79	0.11	0.064	–10.5
--	--	--	–3.20	44	143	0.74	0.03	<0.030	–10.6
--	--	--	–2.40	71	568	0.30	--	52.0	–22.5
–15.9	–115	1.00	8.20	42	134	0.75	0.37	0.42	–6.2
–16.3	–118	–1.80	2.30	30	323	0.23	64.0	63.9	15.8
–16.2	–115	0.00	4.80	43	130	0.79	0.82	0.87	–0.7
–15.1	–107	2.20	8.00	280	780	0.86	0.22	1.3	8.4
–15.8	–113	–2.50	1.70	20	460	0.10	11.6	22.4	6.5
–15.9	–115	–1.20	3.20	99	660	0.36	49.3	58.3	11.4
–16.1	–116	–5.00	–2.20	4	28	0.30	0.25	0.32	–25.5
–14.1	–98	–7.60	–7.60	20	61	0.79	<.001	<0.001	7.3
–15.8	–111	0.50	7.10	82	210	0.94	<0.001	<0.001	–2.6
–15.2	–107	1.00	7.00	420	1,200	0.84	8.8	9.0	–11.2
–13.8	–101	2.30	7.10	360	1,000	0.86	0.42	0.43	–6.4
--	--	--	–2.60	22	363	0.15	0.01	<0.030	–14.4
--	--	--	–2.60	22	363	0.15	0.01	<0.030	–14.4
–16.5	–120	–3.70	–0.50	31	308	0.24	--	45.6	–13.9
–16.0	–115	–3.60	0.90	26	89	0.69	0.050	0.083	12.2
		–10.60	–2.80	17	145	0.28	0.41	8.2	–5.3
–15.2	–109	–7.00	–1.80	60	153	0.94	0.12	0.068	0.9
–14.4	–104	–3.40	3.60	22	182	0.29	0.14	4.3	3.8
–16.6	–121	–6.80	–0.80	29	54	1.29	<0.001	<0.001	7.3
–17.0	–123	–8.50	–2.80	17	25	1.63	<0.001	<0.001	4.2
–13.7	–95	–9.60	–2.40	12	61	0.45	0.023	0.24	–1.1
–15.4	–111	–6.60	–3.70	48	195	0.58	0.033	0.44	–8.3
–15.7	–113	–4.20	4.30	60	141	1.02	--	0.079	2.2
–15.7	–113	–4.20	4.30	60	141	1.02	--	0.079	2.2
–15.7	–115	–2.10	6.50	113	285	0.95	--	2.7	12.9
–15.7	–115	–2.10	6.50	113	285	0.95	--	2.7	12.9
–16.0	–116	–3.40	7.30	190	560	0.81	4.2	3.9	–4.4
--	--	–7.7	0.8	454	2,720	0.40	--	1,250	--
–16.1	–118	0.30	10.00	380	930	0.98	7.6	8.1	2.7

Table 1. Chemical and isotopic data for non-mining affected and mining-affected samples collected in the Animas River watershed study area.—Continued

Site Number	Description	Date	Sample type	Cat	Q cfs	Field Spec. Cond. µS/cm	Field pH	Water temp. °C
CC134	Topeka Gulch at mouth	9/9/94	Stream	4	0.19	1,480	6.72	10.1
CC135	Tributary of Ohio Gulch	9/29/94	Stream	4	0.001	980	3.34	9.4
CC22	Prospect Gulch upstream from mouth	11/5/97	Stream	4	0.440	415	3.23	0.1
CC26	Prospect Gulch near mouth	9/8/97	Stream	4	0.56	526	3.22	8.9
CC43	Stream in Prospect Gulch	9/9/97	Stream	4	0.010	370	2.99	9.9
M27	Mineral Creek upstream from South Fork	10/5/95	Stream	4	27	542	4.99	4.4
M34	Mineral Creek at Silverton	10/5/95	Stream	4	48	359	6.90	7.8
MC79	Middle Fork Cement Creek near mouth	9/27/95	Stream	4	7.9	796	4.75	4.7
MC80	Middle Fork Mineral Creek upstream from Bonner mine	9/30/95	Stream	4	10	727	4.89	5.7
MC88	Middle Fork Mineral Creek upstream from Red tributary	9/20/95	Stream	4	5.6	778	6.39	6.7
MC89	Middle Fork Mineral Creek downstream from Red tributary	9/20/95	Stream	4	7.2	800	4.58	8.0
MC91	Spring below Independence mine	9/26/95	Spring	4	0.020	594	3.45	2.9
MC92	Spring below Bonner mine	9/26/95	Spring	4	0.15	970	3.12	3.9
MS13	Eveline mine	2/13/97	Adit	4	0.014	493	2.81	3.1
MS15	Forest Queen mine	2/12/97	Adit	4	0.036	883	4.44	7.8
MS15	Forest Queen mine	2/12/97	Adit	4	0.036	883	4.44	7.8
MS19	Joe and Johns mine	9/8/97	Adit	4	0.006	1,087	2.79	9.9
MS35	Unnamed mine in Prospect Gulch	9/25/97	Adit	4	0.002	420	6.86	3.0
MS5	Big Colorado mine	10/18/96	Adit	4	0.016	660	3.17	6.6
MS52	Silver Ledge mine	10/18/96	Adit	4	0.75	1,090	5.70	5.6
MS56	Yukon tunnel	5/15/97	Adit	4	--	956	6.98	14.5
MS59	Galena Queen shaft	9/9/97	Adit	4	--	1,062	2.60	4.2
MS6	Black Hawk mine	10/1/97	Adit	4	0.60	1,020	6.95	7.8
MS60	Hercules shaft	9/9/97	Adit	4	--	1,780	2.35	5.8
MS61	May Day mine	5/15/97	Adit	4	0.030	1,810	2.64	1.1
MS69	Leib's hand auger hole #1	5/15/97	Spring	4	0.100	1,123	2.58	4.4
MS72	Unnamed mine in Topeka Gulch	9/8/94	Adit	4	0.009	1,000	6.95	5.5
MS73	Unnamed mine in Topeka Gulch	9/9/94	Adit	4	0.14	1,720	6.85	5.9
MS74	Unnamed mine in Ohio Gulch	9/28/94	Adit	4	0.001	1,110	2.84	8.2
MS75	Unnamed mine in Ohio Gulch	9/28/94	Adit	4	0.026	1,540	3.57	6.0
MS76	Ruby Trust mine	9/18/95	Adit	4	1.0	560	6.36	7.1
MS77	Paradise Portal	9/28/95	Adit	4	0.60	1,962	5.70	4.6
MS78	unnamed mine in Middle Fork Mineral Creek	9/19/95	Adit	4	0.030	215	5.54	5.3
MS80	Independence mine	9/26/95	Adit	4	0.040	667	3.19	4.0
MS81	Koehler tunnel	9/25/95	Adit	4	0.020	3,520	2.45	2.3
MS82	Junction mine	9/25/95	Adit	4	0.15	3,310	2.50	2.5
MS83	Old Hundred mine in tunnel	8/24/95	Adit	4	0.50	570	6.82	10.2
MS83	Old Hundred mine in tunnel	8/24/95	Adit	4	0.50	570	6.82	10.2
MS84	Old Hundred mine at portal	8/24/95	Adit	4	1.5	590	7.35	15.0
MS84	Old Hundred mine at portal	8/24/95	Adit	4	1.5	590	7.35	15.0
MS85	Klondike mine in tunnel	8/25/95	Adit	4	0.001	500	7.58	1.9
MS85	Klondike mine in tunnel	8/25/95	Adit	4	0.001	500	7.58	1.9
MS86	Klondike mine at portal	8/25/95	Adit	4	0.020	123	6.32	2.7
MS86	Klondike mine at portal	8/25/95	Adit	4	0.020	123	6.32	2.7
MS87	American tunnel inside tunnel	8/22/95	Adit	4	--	3,050	6.16	10.6
MS88	American tunnel at portal	8/22/95	Adit	4	--	2,010	5.98	11.7

Table 1. Chemical and isotopic data for non-mining affected and mining-affected samples collected in the Animas River watershed study area.—Continued

$d^{18}O_{H_2O}$	dD_{H_2O}	$d^{18}O_{SO_4}$	$d^{34}S_{SO_4}$	Calcium mg/L	Sulfate mg/L	Molar Ca/SO_4 ratio	Ferrous iron mg/L	Total iron mg/L	Percent charge balance
–15.6	–116	–0.70	8.90	330	850	0.93	0.90	0.87	–1.0
–12.4	–97	–7.96	–2.60	110	490	0.54	0.001	2.3	–6.7
--	--	–9.4	–3.2	25.5	132	0.46	1.04	3.15	--
–15.6	–113	–5.70	–1.20	29	227	0.30	0.42	26.8	15.7
–15.1	–109	–9.20	–2.30	8	92	0.21	0.043	1.9	18.5
--	--	–0.60	4.90	180	270	1.60	--	5.6	67.2
--	--	–1.50	5.20	130	160	1.95	--	1.5	81.0
–16.0	–116	0.00	4.80	130	430	0.73	15.5	15.6	1.4
--	--	–0.40	4.90	--	410	--	--	12.0	--
–16.2	–116	0.20	5.40	140	430	0.78	9.9	10.4	–13.5
–16.1	–115	–0.70	4.80	130	440	0.71	16.5	18.1	–0.6
–15.8	–116	–0.60	5.60	63	260	0.58	0.58	2.4	–2.0
–16.1	–117	0.20	6.40	110	440	0.60	0.50	4.7	1.2
–16.8	–122	–6.60	–2.60	4	153	0.07	--	14.7	30.2
--	--	–4.20	5.90	133	450	0.71	23.3	24	--
--	--	–4.20	5.90	133	450	0.71	23.3	24	--
–17.0	–123	–7.60	–4.40	2	367	0.01	0.91	60.3	–10.8
–16.2	–117	–6.90	–0.20	79	143	1.32	0.012	<0.03	1.7
–16.1	–116	–6.60	–2.60	64	277	0.55	0.40	1.4	5.0
–15.8	–114	–1.60	7.30	211	518	0.98	11.8	12.3	8.0
–15.5	–111	–0.70	9.70	178	538	0.79	--	0.22	–30.9
–16.7	–121	–7.60	–1.70	7	368	0.05	0.83	60.1	23.5
–14.9	–107	–4.30	6.60	259	600	1.04	0.80	1.2	5.4
–15.9	–115	–8.40	–3.10	3	691	0.01	1.8	118	3.2
–14.5	–113	–9.40	–4.90	27	1,060	0.06	--	189	–61.0
--	--	–10.8	–3.4	9.32	300	0.07	--	37.8	--
–15.8	–116	–1.20	8.00	340	770	1.06	4.0	3.8	0.3
–16.4	–120	0.83	10.60	460	1,100	1.00	11.7	12.0	2.7
–14.9	–109	–11.10	–3.40	26	520	0.12	0.004	78.0	–5.9
–15.9	–117	–4.80	–0.50	180	950	0.45	0.094	13.0	–35.1
–16.6	–121	–3.40	5.20	110	200	1.32	0.46	0.47	9.3
–16.0	–115	–0.50	4.70	400	1,200	0.80	66.5	67.0	8.6
–16.7	–122	–5.80	–1.40	20	83	0.58	9.1	9.4	–0.8
--	--	–0.10	5.80	65	--	--	1.4	12.6	--
--	--	–10.70	–0.40	111	2,720	0.10	27.8	686	41.0
--	--	–9.50	–0.60	144	2,700	0.13	31.7	494	4.4
–15.4	–110	–6.60	–1.20	110	200	1.32	<0.001	0.005	6.4
–15.4	–110	–6.60	–1.20	110	200	1.32	<0.001	0.005	6.4
–15.4	–112	–3.20	4.00	110	210	1.26	<0.001	0.005	7.3
–15.4	–112	–3.20	4.00	110	210	1.26	<0.001	0.005	7.3
–14.6	–103	–5.40	–0.70	98	150	1.57	<0.001	0.006	8.3
–14.6	–103	–5.40	–0.70	98	150	1.57	<0.001	0.006	8.3
–15.4	–110	–5.40	–1.50	23	40	1.38	<0.001	0.005	10.4
–15.4	–110	–5.40	–1.50	23	40	1.38	<0.001	0.005	10.4
–16.3	–117	–4.90	1.90	510	2,100	0.58	114	310	–6.6
–16.1	–117	–2.60	7.80	470	1,300	0.87	27.3	27.0	1.9

Analytical Methods for Dissolved Constituents

Samples collected in 1994–95 were analyzed at the USGS National Water Quality Laboratory in Colorado (URL http://wwwnwql.cr.usgs.gov/, accessed November 2002). Calcium and total iron were determined by inductively coupled plasma–atomic emission spectroscopy, and sulfate was determined by ion chromatography according to methods published by Fishman and others (1994). Samples collected in 1996–99 were analyzed at a USGS research laboratory in Boulder, Colo. Calcium and total iron were determined by inductively coupled plasma–atomic emission spectroscopy, and sulfate was determined by a turbidimetric method using a Hach SulfoVer reagent and Hach DR2000 spectrophotometer. For all years, ferrous iron was determined by a colorimetric method using a Hach 1, 10-phenanthroline reagent and Hach DR2000 spectrophotometer. The quality of laboratory analyses was assessed through the analysis of laboratory blanks, sample replicates, USGS standard reference water samples (URL http://btdqs.usgs.gov/srs/, accessed November 2002), and calculated ion balances. Stable isotopes of water ($\delta^{18}O$ and δD) were analyzed at the USGS stable isotope laboratory in Reston, Va. (URL http://isotopes.usgs.gov/index.htm/, accessed November 2002).

Analytical Methods for Oxygen and Sulfur Isotopes of Dissolved Sulfate

One-liter samples collected for sulfate isotopes were pumped through two sequential columns using a peristaltic pump at a flow rate of 4 mL per minute. The first column was filled with a chelating resin (BioRad Chelex 100) and was used to remove iron from solution, because iron can act as an interferant during the isotope analyses (C. Janik, oral commun., 1994). The second column was filled with a NaCl-saturated anion exchange resin (BioRad AG 1-X8 anion-exchange resin, 200–400 mesh), which was used to collect 40 mg of sulfate from each sample. After the sample was pumped through both columns, sulfate was eluted from the anion exchange column using 0.4 M KCl, then precipitated as $BaSO_4$ by adding saturated $BaCl_2$ to the eluent, and heated to enhance crystallization of the precipitate. The $BaSO_4$ precipitate was collected on a membrane filter and air dried prior to analysis. Oxygen and sulfur isotopic analyses were performed on the $BaSO_4$ precipitate by isotope-ratio mass spectrometry at the USGS stable isotope laboratory in Menlo Park, Calif., in 1994 and in Denver, Colo., from 1995 to 1999. Oxygen isotopes of dissolved sulfate are expressed in per mil (parts per thousand) relative to the Vienna Standard Mean Ocean Water (VSMOW) on a scale that is normalized such that the $\delta^{18}O$ of the Standard Light Arctic Precipitation (SLAP) water is –55.5 per mil exactly (Coplen, 1996). The $\delta^{34}S$ of dissolved sulfate are expressed in per mil relative to Cañon Diablo troilite (CDT) standard. Precision of the analyses is ±0.2 per mil.

Analytical Methods for Oxygen and Sulfur Isotopes of Minerals

Pyrite, gypsum, and anhydrite were purified by hand picking. Gypsum and anhydrite were dissolved in distilled water, filtered, and the dissolved sulfate precipitated as $BaSO_4$ with addition of $BaCl_2$ with heating after acidification with HCl to pH 3. Isotopic compositions of sulfur-bearing minerals were made by several methods over the course of the study. Initial sulfur isotope analyses of $BaSO_4$ precipitates and pyrite were made using conventional methods for the preparation of SO_2 gas (Yanagisawa and Sakai, 1983) with analyses on a 6-60 RMS Nuclide Corporation mass spectrometer with a modified source, collector, and pumping system. Later sulfur-isotope measurements were made on a Micromass Optima mass spectrometer using continuous flow methods similar to those described by Giesemann and others (1994). Initial oxygen-isotope analyses of sulfates were made on CO_2 prepared using a BrF_5 technique described by Wasserman and others (1992). Later $BaSO_4$ samples were analyzed as CO by continuous flow methods using a high-temperature pyrolysis device on a Thermo Finnigan Delta Plus mass spectrometer.

Results and Discussion

Seventeen pyrite samples were analyzed for $\delta^{34}S$ and 4 gypsum and 2 anhydrite samples were analyzed for both $\delta^{34}S$ and $\delta^{18}O_{SO_4}$. Results of these analyses are shown in table 2. The distinct isotopic signatures between the pyrite and the gypsum/anhydrite samples can be clearly seen in figure 2. The $\delta^{34}S$ of the pyrite ranges from +2.5 to –6.9 per mil, whereas those for gypsum and anhydrite samples vary from +15 to +18 per mil. This large separation in sulfur isotopic composition provides a useful tracer for estimating the amounts of gypsum/anhydrite dissolution and pyrite oxidation contributing to sulfate in water from the study area, but these results also confirm that the gypsum/anhydrite is of hypogene origin, and not from reaction of acid sulfate waters with calcite or plagioclase during weathering.

Ninety water samples were collected for $\delta^{34}S_{SO_4}$ determinations, and most of these were also analyzed for $\delta^{18}O_{SO_4}$, δD, $\delta^{18}O_{H_2O}$, discharge, specific conductance, pH, temperature, and inorganic constituents. The results used for interpretations in this report are compiled in table 1. For the purposes of this discussion, only the calcium, sulfate, and iron concentrations are reported here. The complete analyses of dissolved inorganic constituents for these samples are given in Sole and others (this volume, Chapter G).

Table 2. Sulfur and oxygen isotopic data for sulfide and sulfate minerals in the study area.

Sample No.	Mineralization area[1]	Mineral	Mineralogical notes[2]	$\delta^{34}S$	$\delta^{18}O_{SO4}$
B1-1918AN	American tunnel	anhydrite	Vein anhydrite, 1,918' below American tunnel	17.3	–3.3
B1-1900	American tunnel	anhydrite	Vein anhydrite, 1,900' below American tunnel	18.0	1.1
B1-1685	American tunnel	gypsum	Coarse, clear vein gypsum, 1,685' below American tunnel.	16.7	–1.9
PPSO4-1	Mount Moly	gypsum	White, fine-granular, vein margin at Paradise portal	14.6	4.7
NSM-1	Near South Silverton	gypsum	Coarse, clear vein gypsum; adjacent to QSP margin	15.2	1.1
TG-1	Ohio Peak–Anvil Mountain	gypsum	Coarse, clear vein? gypsum; mine dump lower Topeka Gulch.	17	3.6
B1-1918PY	American tunnel	pyrite	Fine-grained pyrite in vein with anhydrite, 1,918' below American tunnel.	–1.6	--
SDY3997	Mount Moly	pyrite	Fine blebs of 1–2 mm disseminated pyrite in QSP zone.	2.5	--
SDY05A97	Mount Moly	pyrite	Fine blebs of 1–2 mm disseminated pyrite in QSP zone.	0.7	--
SDPH01PY	Mount Moly	pyrite	Medium-grained pyrite, fracture in hyd prop zone	0.9	--
SDY10B98	Mount Moly	pyrite	Medium-grained pyrite in qtz vein central QSP zone	–3.1	--
BONNERPY	Mount Moly	pyrite	Late-stage pyrite in 3 mm vein	2.0	--
SDB39	Ohio Peak–Anvil Mountain	pyrite	Finely disseminated pyrite, QSP zone, mid Topeka Gulch.	–2.3	--
SDB38	Ohio Peak–Anvil Mountain	pyrite	Finely disseminated pyrite, QSP zone, mid Topeka Gulch.	–5.4	--
IDB61B	Red Mountains	pyrite	Finely disseminated pyrite, QSP zone Prospect Gulch.	–1.5	--
IDB40	Red Mountains	pyrite	Finely disseminated pyrite, QSP zone Prospect Gulch.	–1.7	--
IDB98	Red Mountains	pyrite	Finely disseminated pyrite, QSP zone Prospect Gulch.	–4.7	--
IDB04PY	Red Mountains	pyrite	Finely disseminated pyrite, quartz-pyrophyllite-alunite zone Red Mtn #3.	–5.0	--
HMT-804-602P	Red Mountains	pyrite	Finely disseminated pyrite, quartz-alunite zone 602' beneath upper Lark mine.	–6.9	--
LS998PY	Red Mountains	pyrite	Fine-grained vein pyrite, Lark mine stage 3b (see text).	–3.6	--
LS2BPY	Red Mountains	pyrite	Fine-grained vein pyrite, Lark mine stage 3b (see text).	–3.9	--
GQWSTPY	Red Mountains	pyrite	Fine-grained vein pyrite, Prospect Gulch, above Galena Queen mine, stage 3b (see text).	–2.8	--
GQ498PY	Red Mountains	pyrite	Fine-grained vein pyrite, Galena Queen mine, stage 3b (see text).	–3.4	--

[1]Mount Moly, Ohio Peak-Anvil Mountain, and Red Mountains are names applied to mineralized and altered areas in Bove and others, this volume, Chapter E3. Mount Moly is an informal name applied to the area of peak 3,792 m between Middle and South Forks Mineral Creek.

[2]QSP, quartz-sericite-pyrite; hyd prop, hydrothermal propylitic alteration; qtz, quartz.

Distribution of Stable Sulfate Isotopes for Mined and Unmined Areas

Figure 3 shows the distribution of $\delta^{34}S$ and $\delta^{18}O$ for dissolved sulfate along with some limited data on isotope compositions for gypsum/anhydrite and pyrite. The box suggested for the range of stable isotope composition for gypsum/anhydrite likely extends to the right (towards higher $\delta^{18}O_{SO_4}$), shown by the area outlined by the dashed line, because extrapolation of the mixing trends in the dissolved stable sulfate isotope data indicates it and because two gypsum samples of unknown origin plot in this area of the box. The range of $\delta^{18}O$ for water in the upper Animas River basin is shown as a vertical band on the left side of the diagram and the $\delta^{18}O$ for air (+23.5 per mil) is shown as the right-hand border of the figure. The trend in these data indicates that dissolved sulfate results from a mixture of sulfate from gypsum/anhydrite dissolution and from pyrite oxidation. Note too that as $\delta^{18}O_{SO_4}$ values become lower (more dominated by pyrite oxidation), they also become closer to $\delta^{18}O_{H_2O}$. This trend is consistent with the

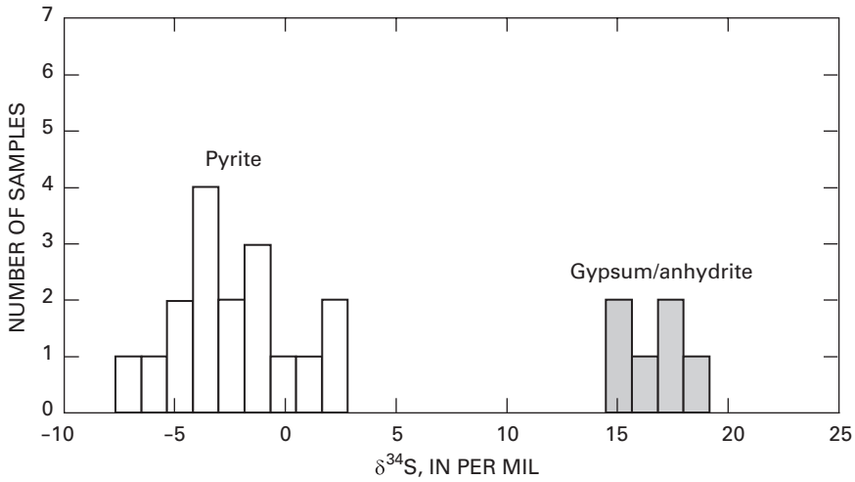

Figure 2. $\delta^{34}S$ values for pyrite and gypsum/anhydrite from Animas River watershed study area.

hypothesis that during pyrite oxidation most of the oxygen in the sulfate comes from water. Indeed, the plot deviates significantly from the diagonal mixing trend for the lowest isotope values where the values trend almost horizontally towards the $\delta^{18}O_{H_2O}$ values. There is also a much greater dispersion in the $\delta^{18}O_{SO_4}$ among the pyrite oxidation-dominated samples, and these isotopically light samples show noticeable overlap between unmined and mining-influenced sites.

Mining-influenced samples are differentiated from those that are not (or are minimally) influenced by mining activities in figure 3, according to a set of established criteria (Mast and others, this volume). A tendency for separation of $\delta^{18}O_{SO_4}$ values from mined compared to unmined environments can be seen, with the samples from unmined areas having higher values. (Although one could interpret the trend alternately in terms of the $\delta^{34}S_{SO_4}$ values being lower, there is no known process by which this pattern could be explained.) The separation at heavier $\delta^{34}S_{SO_4}$ values is likely caused by differences in the isotopic composition of the predominant gypsum/anhydrite dissolving in the basin rather than by different processes of weathering in mined and unmined environments. The tendency for separation among isotopically light samples is not as clear because of notable overlap but is, nevertheless, apparent. A possible reason for this tendency of the isotopic values to separate in the pyrite oxidation-dominated part of the diagram might be the inclusion of more molecular oxygen reacting with the pyrite in the unmined settings compared to the mined settings. However, air has more accessibility in the mined subsurface than in unmined aquifers—and the trend should be in the opposite direction. Qureshi (1986, Ph. D. thesis, University of Waterloo, Waterloo, Ontario, as cited in van Stempvoort and Krouse, 1994) found that as the P_{O_2} increased during laboratory oxidation of pyrite, the resulting sulfate decreased in $\delta^{18}O$. He ascribed this trend to changes in the oxidative pathway and changing importance of intermediate sulfoxyanions during oxidation. Van Stempvoort and Krouse's (1994) comment on Qureshi's results considered the possibility that increasing P_{O_2} may decrease sulfite-water oxygen isotope exchange because the half-life of sulfite would decrease. Decreasing exchange, however, would tend to drive the isotopic composition to heavier values, and consequently, the samples from mined environments should be heavier in isotopic composition than those from the unmined environments. The actual trend (fig. 3) is the opposite from this concept. Alternatively, if the assumption is made that microbially catalyzed oxidation is enhanced in mined environments and, therefore, a much greater concentration of ferric iron is produced in mines, we could conclude that amounts of water oxygen in the sulfate from mined environments should be greater because high ferric iron concentrations use water oxygen in the oxidative pathways.

Although $\delta^{18}O$ values of aqueous sulfate in acidic drainage associated with unmined areas appear to be offset to heavier values relative to mined areas, spatial patterns (combined effects of variations in local geology, mineralogy, elevation, and local hydrology) in isotopic values must also be considered. For example, the Mount Moly alteration area (Bove and others, this volume) has acidic drainage largely unaffected by mining, but it does include a few mines whose water contains $\delta^{18}O_{SO_4}$ values nearly the same as those from the unaffected drainage (fig. 4). If these data were examined alone, the conclusion would be that there is no noticeable isotopic discrimination between drainage from unmined and from mined areas. The effect of spatial differences can be seen better in figure 4 where the data points from figure 3 are shown on an enlarged scale and with different symbols designating the different alteration areas (fig. 1) that have been sampled. Most of the data for both environments in the Mount Moly alteration area group closely together but separately from the Eureka Graben and South Silverton areas. These two distinct but parallel trends suggest that the $\delta^{18}O_{SO_4}$ from dissolving gypsum and anhydrite from the Mount Moly area is just a few per mil heavier than

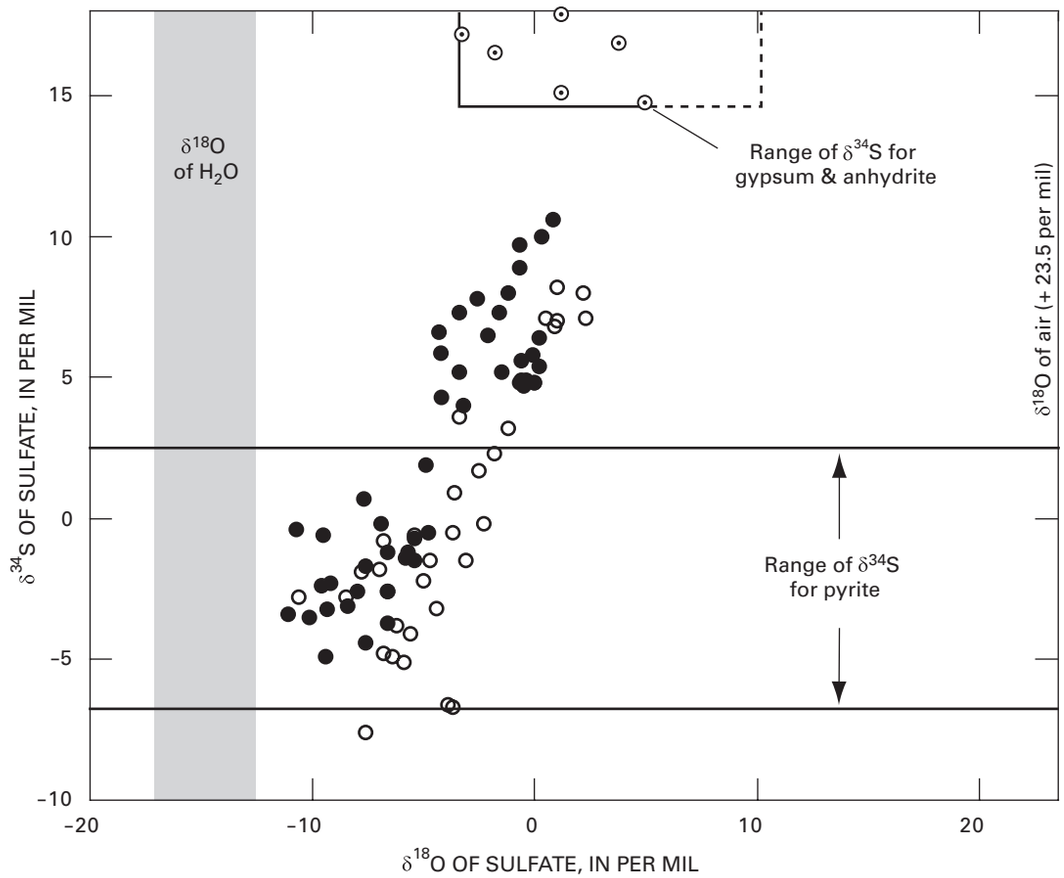

Figure 3. $\delta^{34}S$ of sulfate plotted against $\delta^{18}O$ of sulfate for surface waters in Animas River watershed study area. Open symbols, background water samples; solid symbols, mining-affected water samples; dotted open symbols, gypsum/anhydrite samples. Dashed line, likely extension of range (text, p. 405).

that typical of the other areas. One sample of selenite has been found in this area that has higher $\delta^{34}S_{SO_4}$ and $\delta^{18}O_{SO_4}$ values than do other gypsum samples.

Data for samples from the unmined and mined areas in Topeka and Ohio Gulches (Ohio Peak–Anvil Mountain area) and in the Eureka graben show the best tendency for this separation, and the data for the Prospect Gulch area (Red Mountains area) and the Mount Moly area show the least tendency (or the most overlap). There may be differences in the stable sulfate isotope signatures between undisturbed and mining-influenced drainage, but careful discrimination of the data must be made to properly address this trend based on several factors, including differences of the source gypsum/anhydrite $\delta^{18}O_{SO_4}$ values, pathways of water flow during weathering, and possible effects of pH and aqueous iron redox concentrations. Trends in sulfur and oxygen stable isotopes may follow the same pathways from an intrusive center as changes in mineral zonation and alteration. For example, gypsum and anhydrite are found throughout the watershed except in acid-sulfate alteration zones. Our examination of the data, with regards to zoning, does not warrant further interpretation at this time.

Influence of Gypsum and Anhydrite on Water Chemistry

The influence of gypsum and anhydrite dissolution on water chemistry is shown by figure 5, a plot of calcium concentrations against sulfate concentrations. All samples with $\delta^{34}S_{SO_4}$ greater than +4 per mil are shown by solid circles and those with values less than +4 per mil by open circles. The value of +4 per mil is used as a rough estimate for dividing samples dominated by sulfate from gypsum/anhydrite dissolution versus those dominated by sulfate from pyrite oxidation. Samples with higher sulfur isotope values plot near or on the dissolution line for congruent dissolution of pure gypsum or anhydrite. Indeed, some of the samples closely approach the stoichiometric solubility equilibrium value for gypsum saturation (the stable phase of solid calcium sulfate at temperatures below 56°C). Most of the samples with low calcium:sulfate ratios also have $\delta^{34}S_{SO_4}$ less than +4 per mil, indicating that most of the aqueous sulfate is derived from the only other viable source, pyrite oxidation. If low calcium:sulfate ratios are indicative of pyrite oxidation, then the waters with the lowest

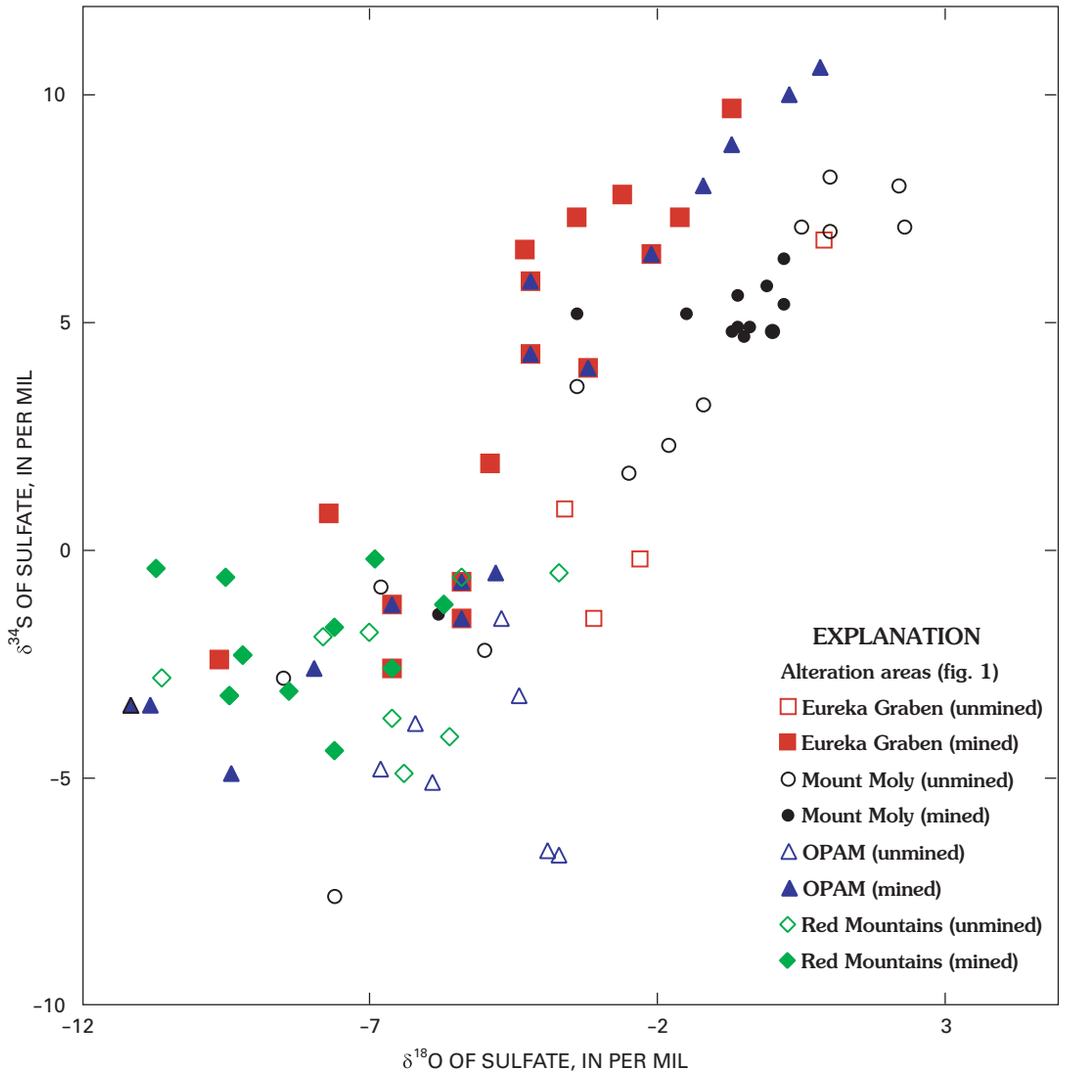

Figure 4. $\delta^{34}S$ of sulfate plotted against $\delta^{18}O$ of sulfate for surface waters in Animas River watershed study area. Symbols designate different alteration areas shown in figure 1. Open symbols represent unmined environments; solid symbols represent mined environments. OPAM, Ohio Peak–Anvil Mountain.

ratios should have the lowest pH values. Figure 6 is a plot of the Ca/SO_4 molar ratio against pH with a solid horizontal line at 1.0 showing ideal gypsum/anhydrite congruent dissolution and an envelope of two dashed lines showing the range of gypsum/anhydrite-dominated dissolution from 0.6 to 1.1. The striking aspect of this plot is that those samples with low Ca/SO_4 ratios (and low $\delta^{34}S_{SO_4}$) all occur at low pH values, nearly all below pH values of 4. The inferred gypsum-dominated samples range in pH from 3 to 7, and those with Ca/SO_4 ratios higher than 1.1 are predominantly at pH values higher than 6, suggesting that calcite dissolution is as important as gypsum dissolution.

Other sulfate minerals known to occur in the watershed include barite, alunite, and jarosite, and these have some potential for contributing to the sulfate concentrations in the water during weathering. These sulfate minerals, however, and most others that may occur are much less soluble than gypsum and anhydrite. Such a large contrast in solubility means that the solubility behavior of barite, alunite, and jarosite will be determined by the concentrations of sulfate produced by the weathering rates of gypsum, anhydrite, and pyrite.

Three Dominant Processes Controlling Water Quality

The preceding trends indicate that three main water types can be classified in the Animas River watershed study area using Ca/SO_4 ratios and $\delta^{34}S_{SO_4}$ values, as shown in figure 7. Each end-member water type represents a major process dominating the water chemistry, and the drawn circles in figure 7 approximately outline these three end-member compositions. The remaining data points between the circles are mixtures between end members. Some of the data points within

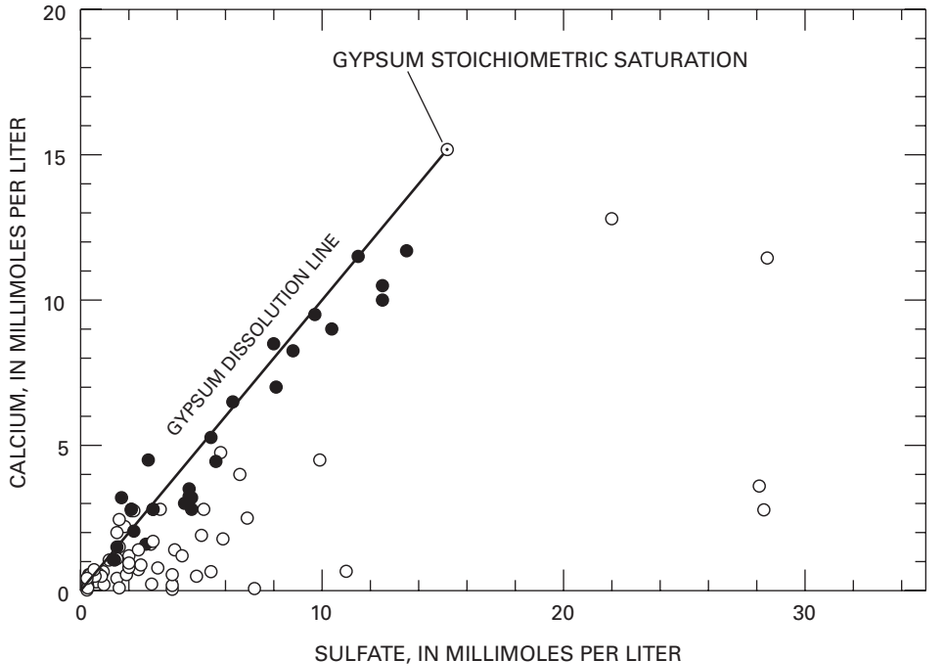

Figure 5. Dissolved calcium versus dissolved sulfate, showing their distribution relative to the congruent dissolution line for pure gypsum (or anhydrite) and the equilibrium solubility value for gypsum in pure water. Solid symbols, water samples with $\delta^{34}S$ greater than +4.0 per mil, indicating a predominance of dissolved gypsum/anhydrite; open symbols, $\delta^{34}S$ <+4.0 per mil.

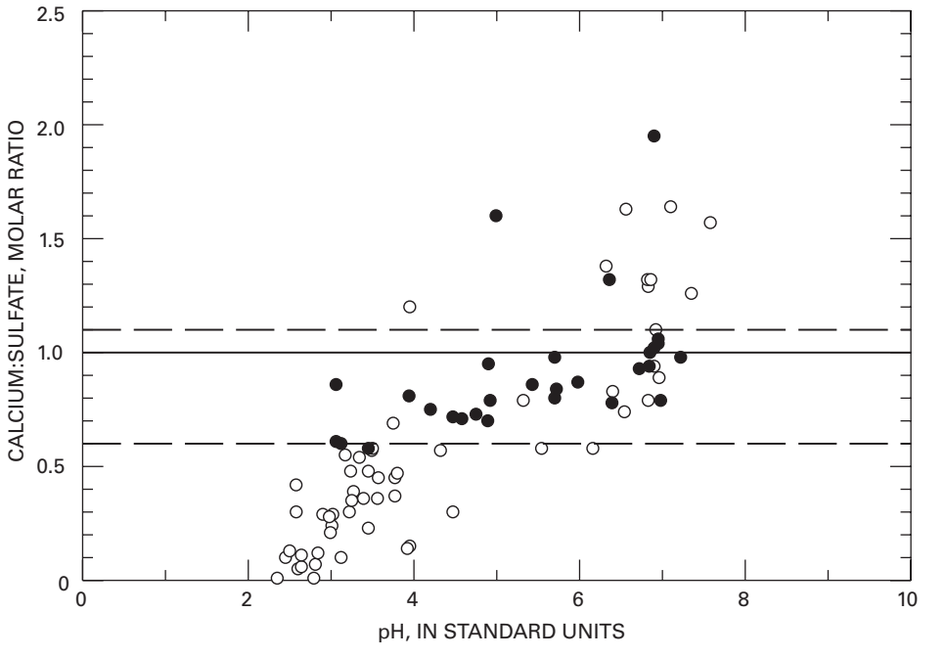

Figure 6. Molar ratio of calcium to sulfate plotted as a function of pH. Solid symbols, samples with $\delta^{34}S$ values greater than +4.0 per mil, as in figure 5; open symbols, $\delta^{34}S$ <+4.0 per mil. Solid horizontal line represents exact gypsum dissolution stoichiometry; two horizontal dashed lines represent approximate range of gypsum-dominated water compositions.

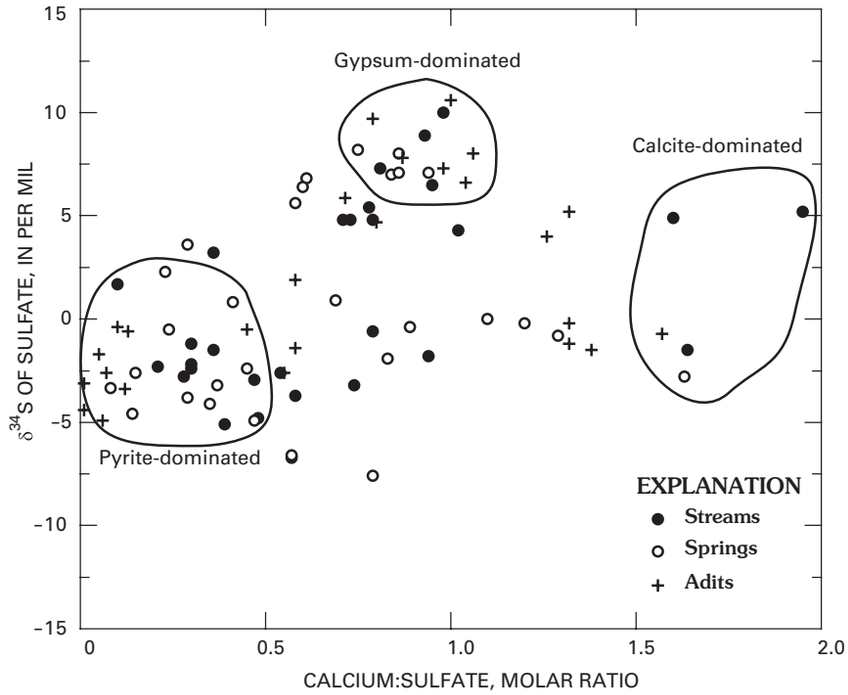

Figure 7. $\delta^{34}S$ of dissolved sulfate in streams, springs, and adits plotted against calcium:sulfate molar ratio.

the drawn circles are also mixtures, and the circles are only shown to help delineate the compositions that are approximately dominated by one of the three processes. One cluster of values appears at low $\delta^{34}S_{SO_4}$ and low Ca/SO_4 ratios, indicative of acid drainage dominated by pyrite oxidation. Another cluster appears at Ca/SO_4 ratios close to 1.0 but with the heaviest $\delta^{34}S_{SO_4}$ values, indicative of gypsum-dominated dissolution. A third, smaller cluster can be seen at intermediate $\delta^{34}S_{SO_4}$ values between that of gypsum dissolution and pyrite oxidation but having the highest Ca/SO_4 ratios, indicating the influence of calcite dissolution in addition to gypsum dissolution. For example, if calcium is solely from calcite and gypsum dissolution in a 1:1 mole ratio, then the Ca/SO_4 ratio would be 2. If the proportion of calcite dissolved was 50 percent of the molar quantity of gypsum dissolved, then the Ca/SO_4 ratio would be 1.5. Figure 7 provides the simplest overall picture of water quality demonstrating the three main processes dominating the water chemistry: (1) pyrite oxidation, (2) gypsum dissolution, and (3) calcite dissolution using only two variables ($\delta^{34}S_{SO_4}$ and Ca/SO_4 ratio).

The plots shown in figures 5, 6, and 7 imply or assume that dissolved aqueous calcium and sulfate behave conservatively; that is, the only reactions that can affect their concentrations are the dissolution of gypsum, anhydrite, and pyrite. Figure 5 shows that the conservative behavior assumption holds because of the consistent linear relationship between calcium and sulfate along the stoichiometric dissolution line for isotopically heavy samples. Although conservative behavior (in the strictest sense for all possible reactions) probably does not hold, the question is whether other side reactions such as the dissolution of plagioclase feldspar, the dissolution of alunite and jarosite, the precipitation of gypsum and calcite, the dissolution of other sulfide minerals (such as chalcopyrite, sphalerite, arsenopyrite), and the dissolution of pyroxenes and amphiboles have any significant effect on the overall mass balance derived from dissolution of gypsum, anhydrite, and pyrite. Based on relative solubilities, relative dissolution rates, relative abundances of minerals in the watershed, and the consistent patterns shown in figures 5–7, the assumption of conservative behavior for calcium and sulfate certainly seems justified in the overall mass balance.

Relationship Between $\delta^{18}O_{SO_4}$ from Pyrite Oxidation and $\delta^{18}O_{H_2O}$

From the previous discussion, the aqueous sulfate samples that are most dominated by pyrite oxidation are clearly those with the lowest pH, the lowest $\delta^{34}S_{SO_4}$ values, and the lowest Ca/SO_4 ratios. This characterization of the data allows the examination of pyrite-dominated samples for the relationship between the water oxygen and the sulfate oxygen. Figure 8 plots all the data for $\delta^{18}O_{SO_4}$ as a function of $\delta^{18}O_{H_2O}$, similar to the type of plot used by Taylor and Wheeler (1994) and van Stempvoort and Krouse (1994). The two diagonal lines are from the study by Gould and others (1989), in which pyrite and other sulfide minerals were allowed to oxidize in the presence of *Acidithiobacillus ferrooxidans* with increasingly

^{18}O-enriched H_2O. Linear equations were derived from the data, and these lines represent the maximum and minimum values from that study. Our data show a range of values somewhat similar to those of other studies, but we have designated those samples with low values of $\delta^{34}S_{SO_4}$ (same as those with low Ca/SO_4 ratios less than 0.6) with open circles to differentiate against the gypsum-dominated samples (solid circles). These samples (open circles) should show the best correlation of $\delta^{18}O_{SO_4}$ with $\delta^{18}O_{H_2O}$; however, they do not. Many of the samples do fall in the range found by Gould and others (1989) and Seal (2003), but a clear positive correlation is not evident in the data. Differentiating the more acidic samples (those with pH <3) does not help, although these do tend to have the lowest $\delta^{18}O_{SO_4}$ values and they are closest to the $\delta^{18}O_{H_2O}$ values. The samples with the highest $\delta^{18}O_{H_2O}$ values are also not the most acidic samples. The tendency for some samples to have higher $\delta^{18}O_{H_2O}$ values suggests that evaporation (or mixing with evaporated waters) may have affected them. Evaporation occurring after sulfate formation would increase the $\delta^{18}O_{H_2O}$ without affecting the $\delta^{18}O_{SO_4}$.

The water isotopes for these samples fall close to the Rocky Mountain meteoric water line (M.A. Mast, unpub. data, 2002) shown in figure 9. Figure 9*B* is an enlargement of the Animas River watershed study area samples and indicates that at least two samples were affected by evaporation. One of these two samples corresponds to the highest $\delta^{18}O_{H_2O}$ in figure 8 (tributary of Ohio Gulch having a low $\delta^{18}O_{SO_4}$). The other sample is the May Day adit sample having a $\delta^{18}O_{H_2O} = -14.5$ ‰ and a $\delta^{18}O_{SO_4} = -9.4$ ‰, the third lowest in $\delta^{18}O_{SO_4}$ shown in figure 8. The next most likely sample to have undergone evaporation is from a sulfide spring in Paradise Basin with $\delta^{18}O_{H_2O} = -13.8$ ‰ and a $\delta^{18}O_{SO_4} = 2.3$ ‰ shown as the highest $\delta^{18}O_{H_2O}$ for a solid circle in figure 8. Some of the other samples may be affected by evaporation to a lesser degree. Overall, no clear trend of $\delta^{18}O_{SO_4}$ can be observed with $\delta^{18}O_{H_2O}$ for aqueous sulfate in samples dominated by pyrite oxidation unless the amount of evaporation and the amount of gypsum or anhydrite dissolution could be determined. Several other processes affect the isotopic composition of the aqueous sulfate from pyrite oxidation such that the $\delta^{18}O_{SO_4}$ values are broadly dependent on $\delta^{18}O_{H_2O}$ but not with respect to specific locations. Mixing of different waters, between the point of pyrite oxidation and the point of sampling, seems likely to change the $\delta^{18}O_{H_2O}$ without changing the $\delta^{18}O_{SO_4}$. Similarly, dilution during snowmelt runoff and major rainstorms and changes in precipitation from one storm to another can change $\delta^{18}O_{H_2O}$ and $\delta^{2}H$ independently of other isotopes.

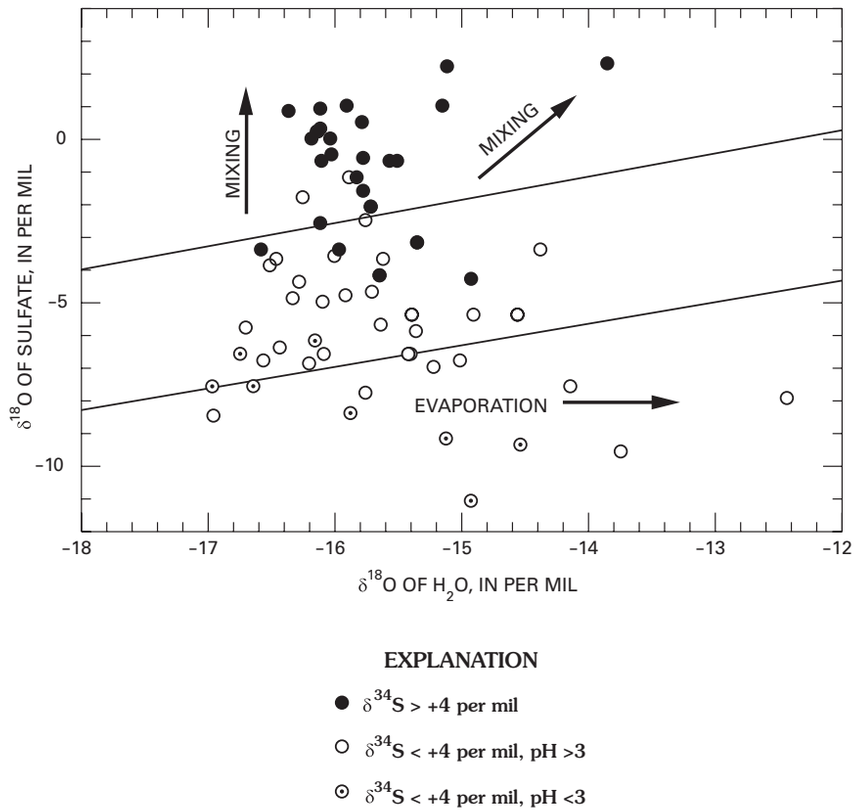

Figure 8. $\delta^{18}O$ of sulfate plotted against $\delta^{18}O$ of H_2O, showing no dependence on water oxygen but possible dispersion of values at low pH due to evaporation. High values of $\delta^{18}O$ of sulfate indicate influence from gypsum/anhydrite dissolution or mixing with such waters. Diagonal lines are based on experimental data from Gould and others (1989).

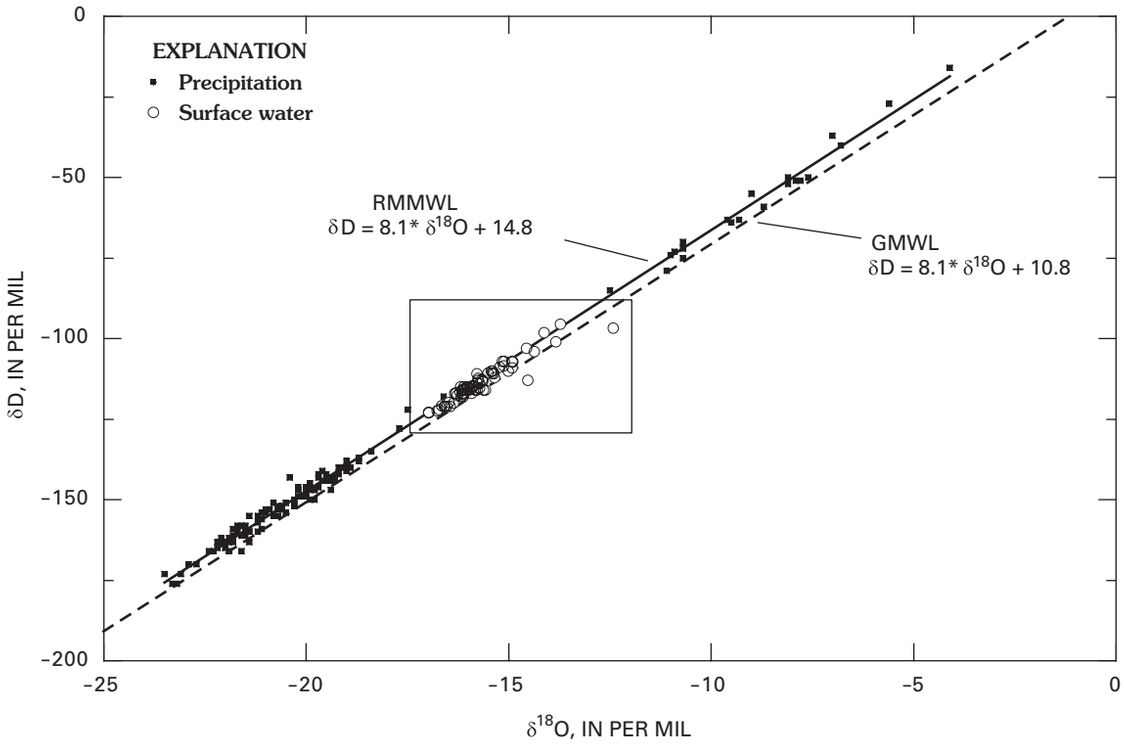

A

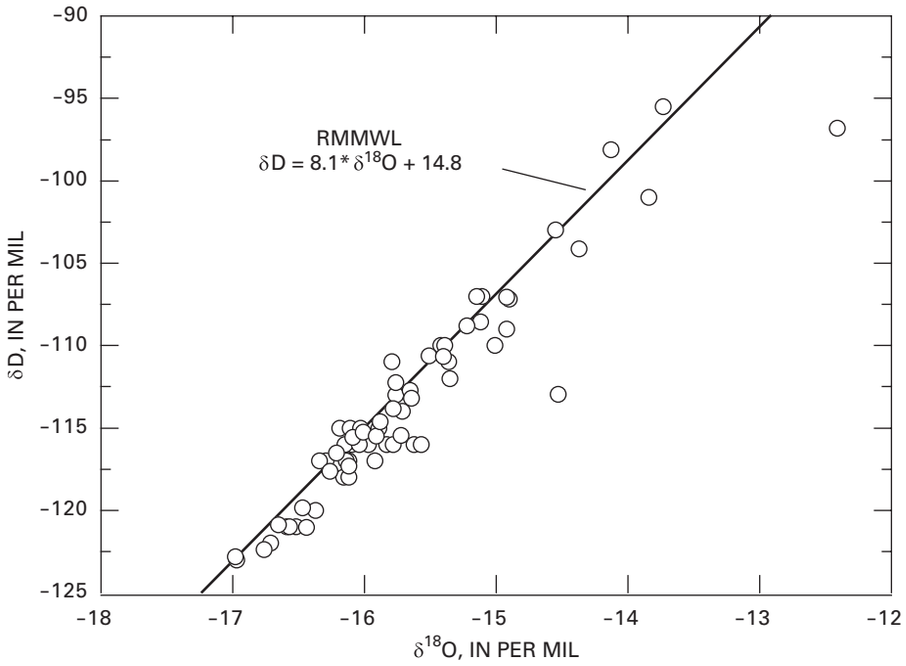

B

Figure 9. $\delta^{18}O$ versus δD of *A*, surface waters collected in Animas River watershed study area and precipitation collected in the Rocky Mountain region, shown with global meteoric water line (GMWL) and Rocky Mountain meteoric water line (RMMWL). *B*, Inset of upper graph, showing only surface water samples collected in study area, with RMMWL. GMWL is taken from Clark and Fritz (1997).

Conclusions

Analysis of more than 100 samples of waters and minerals for sulfur and oxygen isotopes in the Animas River watershed study area, coupled with interpretation, leads to several conclusions. Sulfur and oxygen isotope compositions of aqueous sulfate show a distinct mixing trend from those waters dominated by sulfate production from pyrite oxidation to those dominated by gypsum and (or) anhydrite dissolution. Some discrimination between non-mining affected acid-rock drainage and mining-influenced drainage is apparent in the data for two of the four areas studied in detail, but these differences may be more related to local compositions of primary hydrothermal sulfates than to geochemical processes related to weathering. In the study area, the isotopes show that the gypsum/anhydrite occurrences must be largely of hypogene (hydrothermal) origin, not of supergene (weathering) origin. The gypsum/anhydrite isotopic signature is most evident in samples with higher calcium and sulfate concentrations. Because of the nearly stoichiometric concentrations of calcium and sulfate in many samples on a molar basis, gypsum/anhydrite is apparently the primary source of calcium in these waters. Samples with low calcium:sulfate ratios have consistently low $\delta^{34}S_{SO_4}$ values, indicating pyrite oxidation as the source of aqueous sulfate for the more acidic samples. A few samples show higher calcium:sulfate ratios than would be expected for gypsum/anhydrite dissolution, indicating the importance of calcite dissolution. The sulfur isotopes combined with calcium:sulfate ratios prove to be a simple and useful way to classify these waters into three main end members: gypsum/anhydrite-dissolution dominated, pyrite-oxidation dominated, and calcite-dissolution dominated. Attempts to relate the $\delta^{18}O_{SO_4}$ in the pyrite-oxidation dominated waters to $\delta^{18}O_{H_2O}$ were not successful. Most likely several other processes affect $\delta^{18}O_{H_2O}$ without affecting the $\delta^{18}O_{SO_4}$, including evaporation and the mixing of different $\delta^{18}O$ waters along the flow path before they were sampled.

References Cited

Alpers, C.N., Rye, R.O., Nordstrom, D.K., White, L.D., and King, B.S., 1992, Chemical, crystallographic, and stable isotope properties of alunite and jarosite from acid-hypersaline Australian lakes: Chemical Geology, v. 96, p. 203–226.

Bailey, L.K., and Peters, Ernest, 1976, Decomposition of pyrite in acids by pressure leaching and anodization—The case for an electrochemical mechanism: Canadian Metallurgical Quarterly, v. 15, p. 333–334.

Betts, R.H., and Voss, R.H., 1970, The kinetics of oxygen exchange between sulfite ion and water: Canadian Journal of Chemistry, v. 48, p. 2035–2041.

Bergholm, Anders, 1955, Oxidation av pyrit [Oxidation of pyrite]: Jernkontorets Annallen v. 139, p. 531–541 [translated from the Swedish *in* Baxter, Douglas, Nordstrom, D.K., DeMonge, J.M., and Lövgren, Lars, 1995, U.S. Geological Survey Open-File Report 95–389, 20 p.].

Biegler, T., and Swift, D.A., 1979, Anodic behaviour of pyrite in acid solution: Electrochimica Acta, v. 24, p. 415–420.

Bourda, M.J., Elsetinow, A.R., Schoonen, M.A.A., and Strongin, D.R., 2001, Pyrite-induced hydrogen peroxide formation as a driving force in the evolution of photosynthetic organisms on an early Earth: Astrobiology, v. 1, p. 283–288.

Bourda, M.J., Elsetinow, A.R., Strongin, D.R., and Schoonen, M.A.A., 2003, A mechanism for the production of hydroxyl radical at surface defect sites on pyrite: Geochimica et Cosmochimica Acta, v. 67, p. 935–939.

Brandt, C., and van Eldik, R., 1998, Kinetics and mechanism of the iron(III)-catalyzed autooxidation of sulfur(IV) oxides in aqueous solution—The influence of pH, medium and aging: Transition Metal Chemistry, v. 23, p. 667–675.

Burbank, W.S., and Luedke, R.G., 1969, Geology and ore deposits of the Eureka and adjoining districts, San Juan Mountains, Colorado: U.S. Geological Survey Bulletin 1364, 73 p.

Chibai, Hitoshi, and Sakai, Hitoshi, 1985, Oxygen isotope exchange rate between dissolved sulphate and water at hydrothermal temperatures: Geochemica et Cosmochimica Acta, v. 49, p. 993–1000.

Clark, Ian, and Fritz, Peter, 1997, Environmental isotopes in hydrology: Boca Raton, Fla., Lewis Publishers, 328 p.

Coplen, Tyler, 1996, New guidelines for reporting stable hydrogen, carbon, and oxygen isotope-ratio data: Geochimica et Cosmochimica Acta, v. 60, p. 3359–3360.

Cunningham, C.G., Rye, R.O., Rockwell, B.W., Kunk, M.J., and Councell, T.B., 2005, Supergene destruction of a hydrothermal replacement alunite deposit at Big Rock Candy Mountain, Utah—Mineralogy, spectroscopic remote sensing, stable isotope and argon age evidences: Chemical Geology, v. 215, p. 317–337.

Cunningham, P.T., Holt, B.D., Johnson, S.A., Drapcho, D.L., and Kumar, R., 1984, Acidic aerosols—Oxygen-18 studies of formation and infrared studies of occurrence and neutralization, *in* Durham, J.L., ed., Chemistry of particles, fogs and rain: Boston, Butterworth, p. 53–130.

de Jong, G.A.H., Hazeu, W., Bos, P., Keunen, J.G., 1997, Polythionate degradation by tetrathionate hydrolase of *Thiobacillus ferrooxidans*: Microbiology, v. 143, p. 499–504.

Druschel, G.K., Hamers, R.J., and Banfield, J.F., 2003, Kinetics and mechanism of polythionate oxidation to sulfate at low pH by O_2 and Fe^{3+}: Geochimica et Cosmochimica Acta, v. 67, p. 4457–4469.

Druschel, G.K., Hamers, R.J., Luther, G.W., III, and Banfield, J.F., 2003, Kinetics and mechanism of trithionate and tetrathionate oxidation at low pH by hydroxyl radicals: Aquatic Geochemistry, v. 9, p. 145–164.

Eggelston, C.M., Ehrhardt, J.J., and Stumm, Werner, 1996, Surface structural controls on pyrite oxidation kinetics—An XPS-UPS, STM, and modeling study: American Mineralogist, v. 81, p. 1036–1056.

Eigen, M., Kusten, K., and Maas, A., 1961, Die Geschwindegkeit der Hydration von SO_2 in Wassriger Lösung: Zeitschrift der physikalische Chemie, v. 30, p. 130–138.

England, K.E.R., Charnock, J.M., Pattrick, R.A.D., and Vaughn, D.J., 1999, Surface oxidation studies of chalcopyrite and pyrite by glancing-angle X-ray absorption spectroscopy (REFLEXAFS): Mineralogical Magazine, v. 63, p. 559–566.

Ermakov, A.N., Poskrebyshev, G.A., Purmal, A.P., 1997, Sulfite oxidation—The state-of-the-art of the problem: Kinetics and Catalysis, v. 38, p. 295–308.

Faure, Gunther, 1986, Isotope geology, Second Edition: New York, John Wiley, 589 p.

Field, C.W., 1966, Sulfur isotopic method for discriminating between sulfates of hypogene and supergene origin: Economic Geology, v. 61, p. 1428–1435.

Fishman, M.J., Raese, J.W., Gerlitz, C.N., and Husband, R.A., 1994, U.S. Geological Survey approved inorganic and organic methods for the analysis of water and fluvial sediment, 1954–94: U.S. Geological Survey Open-File Report 94–351, 55 p.

Friederich, C.G., 1998, Physiology and genetics of sulfur-oxidizing bacteria: Advances in Microbial Physiology, v. 39, p. 235–289.

Garrels, R.M., and Thompson, M.E., 1960, Oxidation of pyrite by iron sulfate solutions: American Journal of Science, v. 260, p. 57–66.

Giesemann, A., Jager, H.J., Norman, A.L., Krouse, H.R., and Brand, W.A., 1994, On-line sulfur isotope determinations using an elemental analyzer coupled to a mass spectrometer: Analytical Chemistry, v. 66, p. 2816–2819.

Goldhaber, M.B., 1983, Experimental study of metastable sulfur oxyanion formation during pyrite oxidation at pH 6–9 and 30°C: American Journal of Science, v. 283, p. 193–217.

Gould, W.D., McCready, R.G.L., Rajan, S., and Krouse, H.R., 1989, Stable isotope composition of sulphate produced during bacterial oxidation of various metal sulphides, *in* Biohydrometallurgy—Proceedings of the international symposium held at Jackson Hole, Wyoming, August 13–18, 1989, CANMET Report SP89–10: Warrendale, Pa., The Minerals, Metals, and Materials Society, p. 81–91.

Hall, N.F., and Alexander, O.R., 1940, Oxygen exchange between anions and water: Journal of the American Chemical Society, v. 62, p. 3455–3462.

Hoering, T.C., and Kennedy, J.W., 1957, The exchange of oxygen between sulfuric acid and water: Journal of the American Chemical Society, v. 79, p. 56–60.

Holt, B.D., Cunningham, P.T., Engelkemeir, A.G., Graczyk, D.G., and Kumar, R., 1983, Oxygen-18 study of the nonaqueous-phase oxidation of sulfur dioxide: Atmospheric Environment, v. 17, p. 625–632.

Holt, B.D., Kumar, R., and Cunningham, P.T., 1981, Oxygen-18 study of the aqueous phase oxidation of sulfur dioxide: Atmospheric Environment, v. 15, p. 557–566.

Jambor, J.L., Blowes, D.L., and Ritchie, A.I.M., eds., 2003, Environmental aspects of mine wastes: Ottawa, Mineralogical Association of Canada Short Course Series, v. 31, 430 p.

Kelly, D.P., 1982, Biochemistry of the chemolithotrophic oxidation of inorganic sulfur: Philosophical Transactions of the Royal Society, London, Biology, v. 298, p. 499–528.

Kelly, D.P., 1999, Thermodynamic aspects of energy conservation by chemolithotrophic sulfur bacteria in relation to the sulfur oxidation pathways: Archives of Microbiology, v. 171, p. 219–229.

Kelly, D.P., and Wood, A.P., 2000, Reclassification of some species of *Thiobacillus* to the newly designated genera *Acidithiobacillus* gen. nov., *Halothiobacillus* gen. nov. and *Thermithiobacillus* gen. nov.: International Journal of Systematic and Evolutionary Microbiology, v. 50, p. 511–516.

Krouse, H.R., Gould, W.D., McCready, R.G.L., and Rajan, S., 1991, ^{18}O incorporation into sulphate during the bacterial oxidation of sulphide minerals and the potential for oxygen isotope exchange between O_2, H_2O and oxidized sulphur intermediates: Earth and Planetary Science Letters, v. 107, p. 90–94.

Krouse, H.R., and Mayer, Bernhard, 2000, Sulphur and oxygen isotopes in sulphate, Chapter 7 *in* Cook, P.G., and Herczeg, A.L., eds., Environmental tracers in subsurface hydrology: Boston, Kluwer Academic Publishers, p. 195–231.

Lloyd, R.M., 1967, Oxygen-18 composition of oceanic sulfate: Science, v. 156, p. 1228–1231.

Lloyd, R.M., 1968, Oxygen isotope behavior in the sulfate-water system: Journal of Geophysical Research, v. 73, p. 6099–6110.

Lowson, R.T., 1982, Aqueous oxidation of pyrite by molecular oxygen: Chemical Reviews, v. 82, p. 461–497.

Luther, G.W., 1987, Pyrite oxidation and reduction—Molecular orbital theory considerations: Geochimica et Cosmochimica Acta, v. 51, p. 3193–3199.

Luther, G.W., 1990, The frontier-molecular-orbital theory approach in geotechnical processes, *in* Stumm, Werner, ed., Aquatic chemical kinetics: New York, John Wiley, p. 173–198.

Madigan, M.T., Martinko, J.M., and Parker, Jack, 2000, Brock biology of microorganisms, Ninth Edition: Englewood Cliffs, N.J., Prentice Hall, 1038 p.

Millero, F.J., 2001, The physical chemistry of natural waters: New York, Wiley-Interscience, 654 p.

Mizutani, Y., and Rafter, T.A., 1969, Bacterial fractionation of oxygen isotopes in the reduction of sulphate and in the oxidation of sulphur: New Zealand Journal of Science, v. 12, p. 60–68.

Moses, C.O., and Herman, J.S., 1991, Pyrite oxidation at circumneutral pH: Geochimica et Cosmochimica Acta, v. 55, p. 471–482.

Moses, C.O., Nordstrom, D.K., Herman, J.S., and Mills, A.L., 1987, Aqueous pyrite oxidation by dissolved oxygen and by ferric iron: Geochimica et Cosmochimica Acta, v. 51, p. 1561–1571.

Nesbitt, H.W., and Muir, I.J., 1994, X-ray photoelectron spectroscopic study of a pristine pyrite surface reacted with water vapour and air: Geochimica et Cosmochimica Acta, v. 58, p. 4667–4679.

Nordstrom, D.K., 1982, Aqueous pyrite oxidation and the consequent formation of secondary iron minerals, Chapter 2 *in* Kittrick, J.A., Fanning, D.S., and Hossner, L.R., eds., Acid sulfate weathering: Soil Science Society of America Special Publication 10, p. 37–56.

Nordstrom, D.K., 2000, Advances in the hydrogeochemistry and microbiology of acid mine drainage: International Geology Review, v. 42, p. 499–515.

Nordstrom, D.K., 2004, Modeling low-temperature geochemical processes, Chapter 5.02 *in* Drever, J.I., ed., Surface and ground water, weathering, and soils, Volume 5, H.D. Holland and K.K. Turekian, exe. eds., Treatise of geochemistry: Amsterdam, Elsevier Pergamon, p. 37–72.

Nordstrom, D.K., and Alpers, C.N., 1999, Geochemistry of acid mine waters, *in* Plumlee, G.S., and Logsdon, M.J., eds., The environmental geochemistry of mineral deposits—Part A, Processes, techniques, and health issues: Society of Economic Geologists Reviews in Economic Geology, v. 6A, p. 131–160.

Nordstrom, D.K., and Southam, Gordon, 1997, Geomicrobiology of sulfide mineral oxidation, *in* Banfield, J.F., and Nealson, K.H., eds., Geomicrobiology—Interactions between microbes and minerals: Mineralogical Society of America Reviews in Mineralogy, v. 35, p. 361–390.

Nriagu, J.O., Rees, C.E., Mekhtiyeva, V.L., Lein, A. Yu., Fritz, Peter, Drimmie, R.D., Pankina, R.G., Robinson, R.W., and Krouse, H.R., 1991, Hydrosphere, *in* Krouse, H.R., and Grinenko, V.A., eds., Stable isotopes—Natural and anthropogenic sulphur in the environment: Chichester, U.K., SCOPE 43, Wiley, p. 177–265.

Pearson, R.G., 1976, Symmetry rules for chemical reactions—Orbital topology and elementary processes: New York, John Wiley, 548 p.

Plumlee, G.S., and Logsdon, M.J., eds., 1999, The environmental geochemistry of mineral deposits—Part A, Processes, techniques, and health issues: Society of Economic Geologists Reviews in Economic Geology, v. 6A, 371 p.

Rantz, S.E., and others, 1982, Measurement and computation of streamflow—Volume 1, Measurement of stage and discharge; Volume 2, Computation of discharge: U.S. Geological Survey Water-Supply Paper 2175, 631 p.

Reedy, B.J., Beattie, J.K., and Lowson, R.T., 1991, A vibrational spectroscopic ^{18}O tracer study of pyrite oxidation: Geochimica et Cosmochimica Acta, v. 55, p. 1609–1614.

Rosso, K.M., Becker, Udo, and Hochella, M.F., Jr., 1999, The interaction of pyrite {100} surfaces with O_2 and H_2O—Fundamental oxidation mechanisms: American Mineralogist, v. 84, p. 1549–1561.

Roy, A.B., and Trudinger, P.A., 1970, The biochemistry of inorganic compounds of sulfur: Cambridge, U.K., Cambridge University Press, 399 p.

Rye, R.O., and Alpers, C.N., 1997, The stable isotope geochemistry of jarosite: U.S. Geological Survey Open-File Report 97–88, 28 p.

Rye, R.O., Bethke, P.M., and Wasserman, M.D., 1992, The stable isotope geochemistry of acid sulfate alteration: Economic Geology, v. 87, p. 225–262.

Sand, Wolfgang, Gehrke, Tilman, Jozsa, Peter-Georg, and Schippers, Axel, 2001, (Bio)chemistry of bacterial leaching—Direct vs. indirect bioleaching: Hydrometallurgy, v. 59, p. 159–175.

Sato, Motoaki, 1960, Oxidation of sulfide ore bodies—II, Oxidation mechanism of sulfide minerals at 25°C: Economic Geology, v. 55, p. 1202–1231.

Schippers, Axel, Jozsa, Peter-Georg, and Sand, Wolfgang, 1996, Sulfur chemistry in bacterial leaching of pyrite: Applied and Environmental Microbiology, v. 62, p. 3424–3431.

Schippers, Axel, Rohwerder, T., and Sand, Wolfgang, 1999, Intermediary sulfur compounds in pyrite oxidation—Implications for bioleaching and biodepyritization of coal: Applied Microbiology and Biotechnology, v. 52, p. 104–110.

Schwarcz, H.P., and Cortecci, G., 1974, Isotopic analyses of spring and stream water sulfate from the Italian Alps and Apennines: Chemical Geology, v. 13, p. 285–294.

Seal, R.R., II, 2003, Stable-isotope geochemistry of mine waters and related solids, *in* Jambor, J.L., Blowes, D.L., and Ritchie, A.I.M., eds., Environmental aspects of mine wastes: Ottawa, Mineralogical Association of Canada Short Course Series, v. 31, p. 303–334.

Seal, R.R., II, Alpers, C.N., and Rye, R.O., 2000, Stable isotope systematics of sulfate minerals, *in* Alpers, C.N., Jambor, J.L., and Nordstrom, D.K., eds., Sulfate minerals—Crystallography, geochemistry, and environmental significance: Mineralogical Society of America and Geochemical Society Reviews in Mineralogy and Geochemistry, v. 40, p. 541–602.

Silverman, M.P., 1967, Mechanism of bacterial pyrite oxidation: Journal of Bacteriology, v. 94, p. 1046–1051.

Steger, H.F., and Desjardins, L.E., 1978, Oxidation of sulfide minerals—IV, Pyrite, chalcopyrite and pyrrhotite: Chemical Geology, v. 23, p. 225–237.

Suzuki, Isamu, 1965, Oxidation of elemental sulfur by an enzyme system of *Thiobacillus thiooxidans*: Biochimica et Biophysica Acta, v. 104, p. 359–371.

Taylor, B.E., Wheeler, M.C., and Nordstrom, D.K., 1984a, Isotope composition of sulphate in acid mine drainage as a measure of bacterial oxidation: Nature, v. 308, p. 538–541.

Taylor, B.E., Wheeler, M.C., and Nordstrom, D.K., 1984b, Stable isotope geochemistry of acid mine drainage—Experimental oxidation of pyrite: Geochimica et Cosmochimica Acta, v. 48, p. 2669–2678.

Taylor, B.E., and Wheeler, M.C., 1994, Sulfur- and oxygen-isotope geochemistry of acid mine drainage in the western United States, *in* Alpers, C.N., and Blowes, D.W., eds., Environmental geochemistry of sulfide oxidation: American Chemical Society Symposium Series 550, p. 481–514.

Toran, Laura, 1987, Sulfate contamination in groundwater from a carbonate-hosted mine: Journal of Contaminant Hydrology, v. 2, p. 1–29.

Toran, Laura, and Harris, R.F., 1989, Interpretation of sulfur and oxygen isotopes in biological and abiological sulfide oxidation: Geochimica et Cosmochimica Acta, v. 53, p. 2341–2348.

van Everdingen, R.O., and Krouse, H.R., 1985, Isotope composition of sulphates generated by bacterial and abiological oxidation: Nature, v. 315, p. 395–396.

van Everdingen, R.O., and Krouse, H.R., 1988, Interpretation of isotopic compositions of dissolved sulfates in acid mine drainage, *in* Mine drainage and surface mine reclamation proceedings, Pittsburgh, Pa., April 19–21, 1988, Volume I, Mine water and mine waste: U.S. Bureau of Mines Information Circular 9183, p. 147–156.

van Everdingen, R.O., Shakur, M.A., and Michel, F.A., 1985, Oxygen- and sulfur-isotope geochemistry of acidic groundwater discharge in British Columbia, Yukon, and District of MacKenzie, Canada: Canadian Journal of Earth Sciences, v. 22, p. 1689–1695.

van Stempvoort, D.R., and Krouse, H.R., 1994, Controls of $\delta^{18}O$ in sulfate—Review of experimental data and application to specific environments, *in* Alpers, C.N., and Blowes, D.W., eds., Environmental geochemistry of sulfide oxidation: American Chemical Society Symposium Series 550, p. 446–480.

Wasserman, M.D., Rye, R.O., Bethke, P.M., and Arribas, A. Jr., 1992, Methods for separation and total stable isotope analysis of alunite: U.S. Geological Survey Open-File Report 92–9, 20 p.

Wiersma, C.L., and Rimstidt, J.D., 1984, Rates of reaction of pyrite and marcasite with ferric iron at pH 2: Geochimica et Cosmochimica Acta, v. 48, p. 85–92.

Wilde, F.D., and Radtke, D.B., eds., 1998, National field manual for collection of water-quality data: U.S. Geological Survey Techniques of Water-Resources Investigations, book 9, Chapter A6.

Williamson, M.A., and Rimstidt, J.D., 1993, The rate of decomposition of the ferric-thiosulfate complex in acidic aqueous solutions: Geochimica et Cosmochimica Acta, v. 57, p. 3555–3561.

Xu, Yong, and Schoonen, M.A.A., 1995, The stability of thiosulfate in the presence of pyrite in low-temperature aqueous solutions: Geochimica et Cosmochimica Acta, v. 59, p. 4605–4622.

Yanagisawa, Fumitaka, and Sakai, Hitoshi, 1983, Thermal decomposition of barium sulfate-vanadium pentoxide-silica glass mixtures for preparation of sulfur dioxide in sulfur isotope ratio measurements: Analytical Chemistry, v. 55, p. 985–987.

Zhang, J.-Z., and Millero, F.J., 1994, Kinetics of oxidation of hydrogen sulfide in natural waters, *in* Alpers, C.N., and Blowes, D.W., eds., Environmental geochemistry of sulfide oxidation: American Chemical Society Symposium Series 550, p. 393–409.